THE CONTROL PARAMETERS USED BY THE CNS TO GUIDE THE HAND DEPEND ON THE VISUO-MOTOR TASK: EVIDENCE FROM VISUALLY GUIDED POINTING

L. THALER* AND J. T. TODD

Department of Psychology, The Ohio State University, Columbus, OH 43210, USA

Abstract—To perform visually guided hand movements the visuo-motor system transforms visual information into movement parameters, invoking both central and peripheral processes. Central visuo-motor processes are active in the CNS, whereas peripheral processes are active at the neuromuscular junction. A major share of research attention regarding central visuo-motor processes concerns the question which parameters the CNS controls to guide the hand from one point to another. Findings in the literature are inconsistent. Whereas some researchers suggest that the CNS controls the hand displacement vector, others suggest that it controls final hand position. The current paper introduces a paradigm and analysis method designed to identify the parameters that the CNS controls to guide the hand. We use simulations to validate our analysis in the presence of peripheral visuo-motor noise and to estimate the level of peripheral noise in our data. Using our new tools, we show that hand movements are controlled either in terms of the hand displacement vector or in terms of final hand position, depending on the way visual information relevant for movement production is specified. Interestingly, our new analysis method reveals a difference in central visuo-motor processes, even though a traditional analysis of movement endpoint distributions does not. We estimate the level of peripheral noise in our data to be less than or equal to 40%. Based on our results we conclude that the CNS is flexible with regard to the parameters it controls to guide the hand; that spatial distributions of movement endpoints are not necessarily indicative of central visuo-motor processes; and that both peripheral and central noise has to be carefully considered in the interpretation of movement data. © 2009 IBRO. Published by Elsevier Ltd. All rights reserved.

Key words: hand movements, visuo-motor transformation, execution noise, planning noise, endpoint coding, vector coding.

To perform visually guided hand movements our visuo-motor system performs several computations that are noisy, thus resulting in movement errors. Indeed, many researchers have analyzed movement errors in an effort to determine the computational properties of central and peripheral visuo-motor processes (i.e. Soechting and Flanders, 1989a,b; Soechting et al., 1990; Flanders et al., 1992; Gordon et al., 1994; McIntyre et al., 1997, 1998; Messier and Kalaska, 1997; Harris and Wolpert, 1998; Henriques et al., 1998; Carrozzo et al., 1999; van den Dobbelsteen et al., 2001; Hamilton et al., 2004; van Beers et al., 2004; Vindras et al., 2005; Simmons and Demiris, 2006). Central visuo-motor processes are active in the CNS, whereas peripheral processes are active at the neuromuscular junction (van Beers et al., 2004; Churchland et al., 2006).

Since peripheral noise arises at the neuromuscular junction it depends on physical movement parameters, such as the muscles involved, movement amplitude, direction, speed, etc. It follows that peripheral noise will be the same as long as those parameters are the same. Only recently has a model of peripheral noise been suggested that explains a wide pattern of movement data (van Beers et al., 2004). However, it has also been reported that neuronal activity arising prior to movement onset can predict ~50% of variability in movement speed. Since this neural activity arises before the movement is performed, it indicates the contribution of central visuo-motor processes (Churchland et al., 2006). Based on these results it appears necessary to consider both peripheral and central noise sources in the analysis and interpretation of visuo-motor performance.

With regard to central visuo-motor processes it has been of longstanding interest to determine which parameters the CNS controls to guide the hand. Consider for example the simple task of moving the hand from point A to point B. To perform this task it is possible that the CNS determines the desired goal state of the hand as an end location in space (van den Dobbelsteen et al., 2001), as a goal posture (Rosenbaum et al., 1995; Desmurget and Prablanc, 1997) or as an equilibrium point (Feldman, 1966; Polit and Bizzi, 1979; Bizzi et al., 1984) and that it employs control mechanisms that monitor how the motor apparatus advances toward its desired goal state. Alternatively, it is also possible that the CNS determines the desired distance and direction that the hand has to travel, i.e. the movement vector, and that it employs control mechanisms that monitor how the hand traverses this vector (Bock and Eckmiller, 1986; Gordon et al., 1994; Rossetti et al., 1995; De Graaf et al., 1996; Ghez et al., 1997; Vindras and Viviani, 1998). Even though the difference between these two alternative control schemes appears subtle, it is fundamental. In the first scenario, which is referred to as endpoint coding, movement vectors follow from end positions. In the

*Correspondence to: L. Thaler, Department of Psychology, The University of Western Ontario, Social Science Building, Room 6237, London, Ontario, Canada N6A 5C2. Tel: +519-661-2069; fax: +519-661-3961.
E-mail address: lthaler2@uwo.ca (L. Thaler).
Abbreviations: CNS, central nervous system; 2D, two dimensional; 3D, three dimensional.

second scenario, which is referred to as vector coding, positions follow from movement vectors. Consequently, endpoint coding predicts that errors towards a particular point in space depend on the target, but not on the path that the hand has to traverse. In contrast, vector coding predicts that movement errors will depend on the path the hand has to traverse, rather than on a particular point in space.

Endpoint and vector coding models differ with regard to the visual information that they use to determine the movement goal. Typically, endpoint coding models determine the desired end position of the hand based on visual information in eye or head centered coordinates. By definition, endpoint coding models have to use coordinates that define target position regardless of current hand position. Otherwise, coordinates would specify the hand-target vector, which would render endpoint coding equivalent to vector coding. Vice versa, since vector coding models are based on the idea that the CNS controls the movement vector, they have to use a coordinate system that defines target position with respect to the hand (Bock and Eckmiller, 1986; Vindras and Viviani, 1998). Thus, they cannot use eye-centered coordinates, for example, since distance and direction of the eye-target vector will not match the hand-target vector, unless the movement originates at the eye.

Various methods have been used to investigate if the CNS controls the final position or the displacement vector of the hand. One popular approach is to characterize the shape and orientation of distributions of movement endpoints by means of multivariate gaussian distributions, i.e. by fitting them with an ellipse (in the plane) or with an ellipsoid (in three-space). Results that have been obtained with this method are inconsistent. Distributions that are aligned with the direction of movement can be interpreted as evidence for vector coding (Gordon et al., 1994; Messier and Kalaska, 1997) whereas distributions aligned with the line of sight or the body can be interpreted as evidence for endpoint coding (Soechting and Flanders, 1989a,b; Flanders et al., 1992; McIntyre et al., 1997, 1998; Carrozzo et al., 1999; van den Dobbelsteen et al., 2001). Interestingly, distributions in the plane have the tendency to be aligned with the direction of movement, whereas distributions obtained in three-space have the tendency to be aligned with the line of sight. Based on this observation it has been suggested that subjects employ different central visuo-motor processes, depending on the movement degrees of freedom available (Desmurget et al., 1998). This interpretation is conditional on the assumption that peripheral and perceptual noise do not contribute to differences between distributions of movement endpoints between conditions. However, this assumption is difficult to justify given differences in physical movement characteristics (i.e. speed, curvature, amplitude, etc.) and overall noise magnitude between 2D and 3D paradigms. It is important to point out in this context that peripheral noise will mimic vector coding whenever the movement trajectory is similar to the visual hand-to-target vector (van Beers et al., 2004). This situation might be more likely when movements are performed in the plane. Thus, differences in peripheral noise might be an alternative explanation for differences in endpoint distributions between 3D and 2D paradigms.

Distributions of movement endpoints not only depend on external factors that affect movement degrees of freedom, but also on how visual information is specified (Messier and Kalaska, 1997). For example, when target distance and orientation are specified in the same plane as the movement plane (both horizontal) and subjects can move their hand towards a visible target, errors in movement extent and direction increase at the same rate with movement distance (Messier and Kalaska, 1997). In contrast, when target distance and orientation are presented in the vertical plane, whereas movements are performed in the horizontal plane, such that subjects cannot reach towards a visible target but are forced to mentally transform the visual displacement into a hand movement, errors in movement extent and direction follow different scaling rules (Gordon et al., 1994; Messier and Kalaska, 1997). Independence of errors in movement extent and direction in hand-centered coordinates has been interpreted in favor of the idea that the CNS uses vector coding. However, the finding that extent and direction errors are dependent on when subjects move their hand towards a visible target challenges the generality of this interpretation.

The possibility arises that the way in which visual information is specified, determines how the CNS controls movements. For example, it is possible that subjects control the movement endpoint when they can reach towards a visible location, but that they control the hand displacement vector when they have to explicitly transform the visual displacement vector into a hand movement. However, the contribution of peripheral or perceptual noise must also be considered in this context—e.g. see Messier and Kalaska (1997).

In summary, the literature regarding peripheral and central visuo-motor processes reveals a complex picture with many seemingly discrepant findings (for more complete reviews see Desmurget et al., 1998; Lacquaniti and Caminiti, 1998; Desmurget and Grafton, 2000; Todorov, 2004). Of particular importance in this regard is the question which parameters the CNS controls to guide the hand. Some of the inconsistencies in the literature could potentially be resolved if we assumed that central visuo-motor processes (i.e. hand movement control parameters) adapt to specific task demands. However, as of today the evidence for flexible central visuo-motor processes is inconclusive because peripheral and perceptual noise sources have not been considered as potential confounds.

The current experiments were designed to test if the CNS is flexible in its choice of movement control parameters. We decided to test this hypothesis using a sequential movement paradigm that manipulates the way visual information relevant for movement production was presented to subjects. To analyze our data we extended a method that was introduced by van den Dobbelsteen et al. (2001). This analysis method is potentially more powerful than traditional techniques for distinguishing vector from endpoint coding and may detect differences in central noise properties even when distributions of movement endpoints are undistinguishable. To dem-

onstrate the validity of our analysis in the presence of peripheral noise we modeled both central and peripheral noise processes and applied our analysis to the simulated data. In addition to demonstrating the power of our method, the simulations also enable us to estimate relative proportions of central and peripheral noise in our data and to compare these estimates to neuro-physiological estimates reported elsewhere (Churchland et al., 2006).

EXPERIMENTAL PROCEDURES

Subjects

Eight subjects (six male, two female), including the authors, participated in the experiment. One male subject reported being left-handed and chose to perform the experimental task with his left hand. Subjects gave informed consent before the experiment and were paid for their participation. All subjects had self-reported normal or corrected to normal vision.

Apparatus

A sketch of the experimental apparatus is provided in Fig. 1. Subjects were seated on a height adjustable chair. Stimuli were displayed on a rear projection screen and viewed by subjects in a front-surface mirror that was mounted halfway between the rear projection screen and a digitizing tablet. Subjects moved their hands on the digitizing tablet. Thus, the mirror prevented subjects from seeing their hand during the experiment. Matched distances between mirror surface and screen, and mirror surface and tablet made the mirror reflection of stimuli appear to be in the same plane as the movement plane on the digitizing tablet.

Hand movements were recorded with a hand held stylus on the digitizing tablet (AccuGrid, Model A90; Numonics Corporation, Montgomeryville, PA, USA, 1200(H)×900(V) mm, accuracy 0.254 mm) at a temporal and spatial resolution of 200 Hz and 40 lines/mm, respectively. Stimuli were projected on the rear projection screen with a VGA projector (Casio XJ-360, Casio Computer Co., Ltd, Tokyo, Japan) at a temporal and spatial resolution of 60 Hz and 1024(H)×768(V) pixels, respectively. The active display area sub-

tended 863(H)×647(V) mm. Displays were viewed binocularly in a darkened room and a chin rest was used to avoid changes in head position. Subjects' eyes were located ~460 mm above the tablet. A computer (Dell Dimension 8300 PC, Dell Inc., Round Rock, TX, USA, with an ATI Radeon 9700 PRO graphics card, AMD, Sunnyvale, California, USA) was used to control stimulus presentation and data collection. Before each experimental session, a projected 17-point grid was aligned with a corresponding grid on the rear projection surface to correct changes in lens position that could occur between sessions.

Stimuli and task

Subjects performed sequences of hand movements in two conditions that differed in the type of information that was used to inform subjects of the required hand movement on each trial (Fig. 2). In "Endpoint" conditions, subjects were presented with sequences of visual targets, one target at a time. Targets consisted of black 5 mm diameter circles projected onto the virtual movement surface. Subjects were instructed to move their hand smoothly from one target to the next during a block, so that the endpoint of one movement was the starting point for the next movement. In "Displacement" conditions, subjects were presented with sequences of visual displacement vectors, one at a time. Displacement vectors consisted of one white and one black 5 mm diameter circle projected onto the virtual movement surface. Subjects were instructed to move their hand to a location whose position with respect to the hand starting point was identical to the position of the black dot with respect to the white dot. Just as in "Endpoint" conditions, the endpoint of one movement was the starting point for the next movement. All stimuli were presented in front of a light gray background covered with 2500 small, randomly positioned points. Random positions were recomputed on every block. The main difference between "Endpoint" and "Displacement" conditions is that subjects can reach towards a visible target location in "Endpoint" conditions, but that they have to mentally transform the visual displacement vector into a hand displacement in "Displacement" conditions. However, visual information is always specified at the same scale and in the same plane as the movement plane. We chose this presentation mode because we found previously that perceptual errors in perceived distance are very similar in
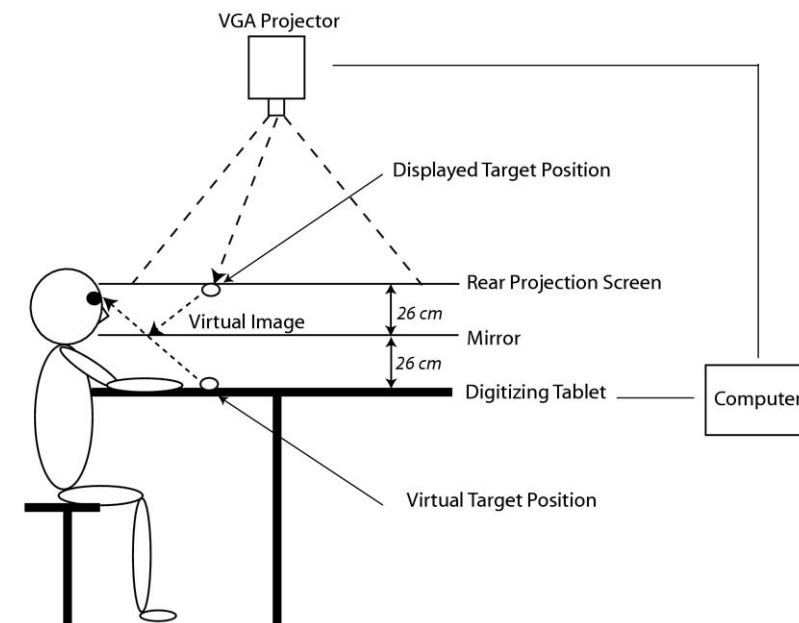

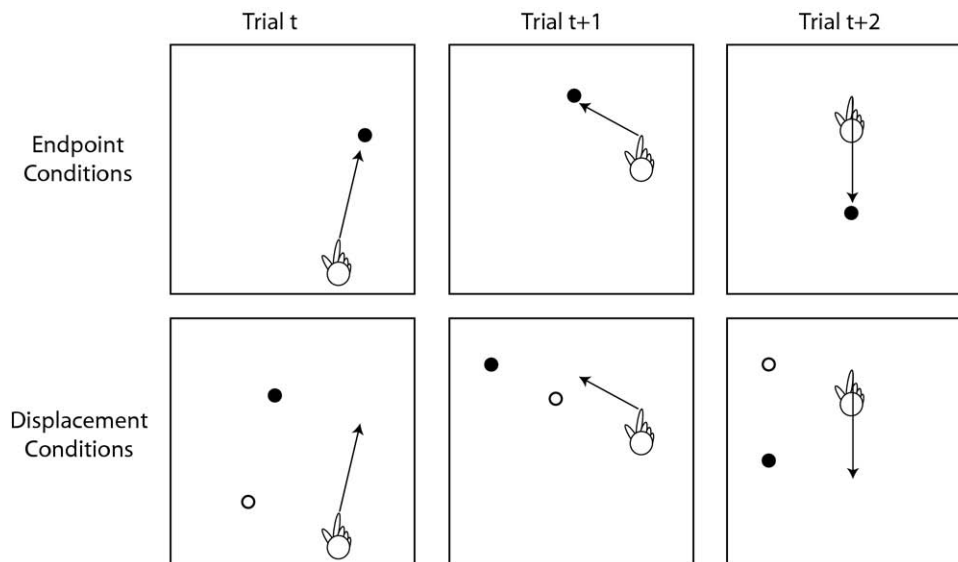Fig. 1. Sketch of the experimental apparatus.

Fig. 2. Illustration of the experimental task performed in "Endpoint" and "Displacement" conditions. In "Endpoint" conditions, subjects were presented with sequences of black target dots, one at a time. Subjects were instructed to move their hand from one target to the next. In "Displacement" conditions, subjects were presented with sequences of visual displacement vectors, one at a time. Subjects were instructed to move their hand from their current position to a location whose position with respect to the hand starting point was identical to the position of the black dot with respect to the white dot.

these two conditions and with the spatial distances tested here (Thaler and Todd, submitted for publication).

Fig. 3 provides a bird's-eye view of the virtual movement surface and the experimental setup for right-handed subjects. The setup was mirror symmetric for the left-handed subject. Targets or visual displacements, respectively, were organized into two different target configurations (Fig.3b, d and c, e) that were presented in different blocks in pseudo-random order. Each configuration consisted of three main coordinates (diamonds in Fig. 3b–e) and four "filler" coordinates (crosses in Fig. 3b–e). Filler coordinates were used to increase the variability of movement paths, but they were traversed less often than main coordinates. Across filler and main coordinates, there were 10 spatially distinct coordinates across both configurations. The three main coordinates in configuration 1 (Fig. 3b, d) formed an equilateral triangle, each side 112.5 mm long. The three main coordinates in configuration 2 (Fig. 3c, e) formed a triangle with side length 150, 112.5 and 75 mm. In "Endpoint" conditions coordinates were presented in pseudorandom order, such that the six possible paths between the three main coordinates of a given configuration and an additional six paths between any main and "filler" coordinates were traversed every 12 movements. In "Displacement" conditions, subjects were presented with visual displacements vectors computed as paths between main and filler coordinates. The white dot of displacement vectors was translated 100 mm to the left and 160 mm to the front with respect to the starting point of the hand. Displacements were presented in pseudorandom order, so that the six possible paths between the three main coordinates of a given configuration and an additional six paths between any main and "filler" coordinates would be traversed every 12 movements.

Procedure

Each block began with the display of the hand starting position and the first target, or displacement vector, respectively. To initiate a block subjects moved their hand to the starting position. During this phase subjects received continuous feedback on hand position via a green cursor dot (3 mm diameter) projected on their real hand position. Once subjects had remained within the 5 mm diameter circle around the starting position for at least 1.8 s, a beep would

indicate the beginning of a block. Synchronous with the beep the on-line hand feedback would disappear, while the target or displacement vector and initial hand starting point would remain visible.

Subjects were instructed to move their hand as accurately as possible in one smooth movement. No instructions were given with respect to the speed of the movement. A movement was considered to have ended when the subject's hand had moved less than 1.5 mm during the last 400 ms. Then, a beep indicated the end of a trial and feedback was given. Thus, subjects received feedback after each single movement. In "Endpoint" conditions, feedback was given via a green cursor dot (3 mm diameter) projected onto the position of the hand. In "Displacement" conditions, the feedback dot was not positioned on the subject's hand, but indicated subjects' moved displacement translated onto the target displacement. Thus, the cursor dot would coincide with the black dot of the displacement, if a subject's movement matched the target displacement. All subjects were aware that the location of the cursor differed from the location of their hand. After 450 ms, another beep would signal the next trial, the next target or target displacement would appear, while the previous target and feedback would disappear. From their current position, subjects then moved smoothly to the new target or over the new target displacement. Subjects were instructed to not move their hand in between trials.

Each block consisted of 49 movements using one of the two possible configurations. The first movement was considered the "starting movement" and during the remaining 48 movements each of the six paths between any two main coordinates was traversed four times (=24 movements) and the additional 24 movements consisted of paths between two filler coordinates. "Endpoint" and "Displacement" conditions were blocked in sessions that subjects performed in direct succession. Order of "Endpoint" and "Displacement" sessions was counterbalanced across subjects. In both "Endpoint" and "Displacement" sessions, each subject performed six blocks, three blocks for each of the two configurations that were presented in pseudorandom order. Thus, each subject gave a total of 2 (conditions)×6 (blocks)×49 (trials)=588 responses and 12 responses were given by each subject to each path between any two main coordinates of a configuration in both "Displacement" and "Endpoint" conditions. In the
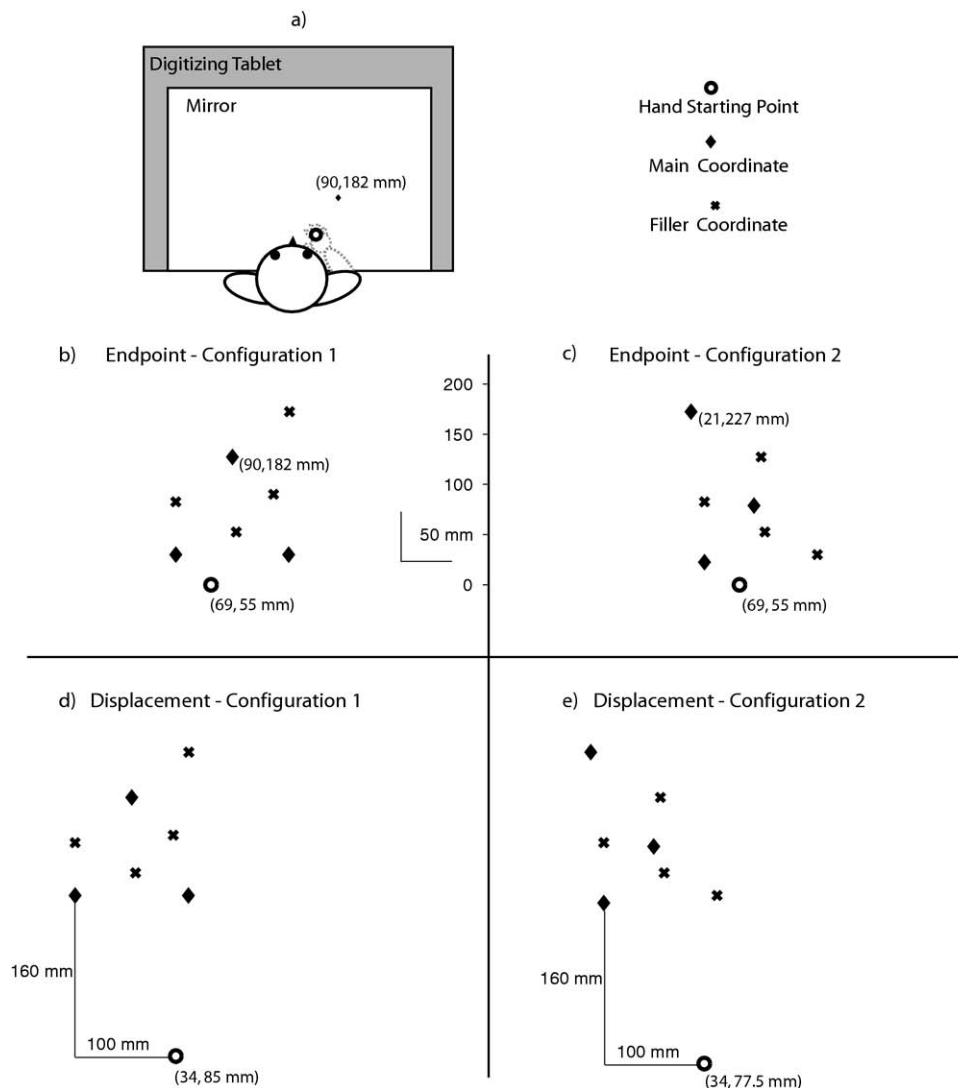
Fig. 3. (a) Bird's-eye view of the (virtual) movement area (not drawn to scale). (b, c) Configurations used in "Endpoint" conditions. In the actual experiment, targets were indicated with black circles. Subjects never saw a complete configuration, but only one target at a time. (d, e) Configurations used in "Displacement" conditions. In the actual experiment, displacements were indicated with white and black circles. Subjects never saw a complete configuration, but only one displacement at a time. Coordinates of hand starting points are given with respect to subjects' eye position. Setup for the left-handed subject was mirror symmetric.

beginning of "Endpoint" and "Displacement" sessions, each subject performed at least 20 practice trials to get familiar with the task. Practice trials were not recorded. Total experimental time was about 50 min per subject. On questioning all subjects reported that both tasks felt quite natural to them.

Data analysis

Analysis of movement kinematics and trajectory shape. There is the possibility that factors such as average movement velocity, peak movement velocity, movement duration and trajectory shape differ between "Endpoint" and "Displacement" conditions. If this was the case, peripheral noise is a potential covariate that would affect our conclusion regarding central visuo-motor processes. As a numerical measure of trajectory shape, we computed the curvedness of smoothed movement traces as the maximum absolute deviation of a point on a trajectory to a straight-line connecting end and start points, divided by trajectory length (At-

keson and Hollerbach, 1985). We multiplied this value by 100 to transform the measure into a percentage—e.g. a value of 50% indicates a semicircular trajectory. Furthermore, we computed the average movement distance, average movement velocity, peak movement velocity and movement duration for all movement traces for each subject. Velocities were obtained by numerical differentiation. All computations were applied to movement trajectories smoothed with a 7 Hz Butterworth filter.

Analysis of distributions of movement endpoints. As a standard analysis, we fit the distributions of movement endpoints using minimum variance ellipses. The analyses were performed for every subject separately. To characterize the shape of the distribution we fitted a minimum variance ellipse to all movement endpoints made along each possible movement path (Gordon et al., 1994; van Beers et al., 2004) by computing the eigenvalues λ and the eigenvectors of the 2×2 sample covariance matrix R, whose elements are given by:

$$R_{jk} = \frac{1}{n}\sum_{i=1}^{n}\delta_{ij}\delta_{ik}$$

where the deviation $\delta_i = \vec{p}_i - \bar{\vec{p}}$ is the endpoint of movement i along one of two orthogonal axes (rows and columns j, k $\subset$ {x, y}) and $\bar{\vec{p}}$ is the mean position over n trials. The square root of the eigenvalues corresponds to the standard deviation of movements along each axis specified by the associated eigenvectors. The aspect ratio of the ellipse was determined by dividing the square root of the larger eigenvalue by the square root of the smaller eigenvalue, i.e. $\sqrt{\lambda 1}/\sqrt{\lambda 2}$. The larger the ratio, the more elongated the ellipse. Ellipse size depends on magnitude of the eigenvalues and computing the SD of movements in the plane is equivalent to computing ellipse area:

$$SD_{2D} = \pi \frac{\sqrt{\lambda 1}}{2}\frac{\sqrt{\lambda 2}}{2}.$$

In addition to computing minimum variance ellipses we also computed standard deviation of movement endpoints in the direction of movement (on-axis errors) and orthogonal to it (off axis errors) and took their ratio (on-axis/off-axis) (Gordon et al., 1994; Messier and Kalaska, 1997). This analysis will yield a different result from the minimum variance ellipse analysis whenever the major axis of the minimum variance ellipse is not oriented in the direction of movement. In the extreme, i.e. when the major axis of the minimum variance ellipse is oriented orthogonal to the direction of movement, the ratio of on- and off-axis errors is the inverse of the aspect ratio of the minimum variance ellipse.

The same analyses was performed for movements in "Displacement" conditions, with the difference that we first aligned movements on those targets that had been used as starting point in the computation of the target displacement. The reason for alignment is that the instruction to subjects to always move over the visual displacement from their current position introduces shifts of subsequent movements in the direction of any preceding error. Alignment removes variability due to those instruction-based shifts.

Control system analysis. In our control system analysis, we tested to what degree subjects use vector and endpoint coding in "Endpoint" and "Displacement" conditions. If subjects use vector coding, movement errors with regard to targets in space should result from errors that depend on the displacement vector of the hand. In contrast, if subjects use endpoint coding, errors with regard to the displacement vector of the hand should result from errors that depend on targets in space. (Assuming that subjects look at the target on every trial and assuming that their head remained stationary in the chinrest, eye- (i.e. line of sight), head- (i.e. cyclopean eye) and body-centered coordinates remain stable throughout our experiment and do not vary with the movement of the hand. Thus, our paradigm and analysis enables us to distinguish between hand- and target-centered control parameters, i.e. between vector and endpoint coding. However, our analysis does not permit us to distinguish between different types of endpoint coding. In principle, our paradigm and analysis could be extended to determine if subjects use eye-, head- or body-centered endpoint coding by incorporating systematic shifts of the gaze, head and body.) Our analysis illustrated in Fig. 4 exploits this logic and is an extension of an analysis introduced by van den Dobbelsteen et al. (2001).

On each trial, subjects move from one target location to another, or over a certain target displacement, respectively. We can decompose each movement (Fig. 4a) into three components: Let us define movement start and endpoints as observed start and observed endpoints (Fig. 4b) and the straight line that joins observed start and ending points as observed movement displacement (Fig. 4g).

To determine to what degree subjects use hand-centered control, i.e. vector coding, in "Endpoint" conditions we followed the steps illustrated in Fig. 4b–f. First, we computed all observed movement start and endpoints made from any other target towards a certain main target (Fig. 4b). Then, we computed SD_{2D} of observed endpoints for a particular main target—across all starting points. This is equivalent to computing movement errors with regard to targets in space (Fig. 4c). Then, we combined observed displacements with start points from other movements. (The combination of a displacement from one trial with the starting point of another assumes that all displacements towards a particular target are planned according to the same visual target displacement. This assumption is not met in our experiment, because subjects moved towards a target from various starting points and because subjects received visual feedback that created a different visual displacement vector on every trial. Thus, it is conceptually incorrect to combine a displacement from one trial with the starting point of another. We therefore did not recombine displacements with starting points (as shown in Fig.4d), but we recombined displacement errors with hand-target vectors instead. The computation of displacement errors and the recombination procedure are described in Appendix A.) This is equivalent to reshuffling errors that depend on the displacement vector of the hand (Fig. 4d). From this recombination, we obtained fictional endpoints (Fig. 4e). If subjects use vector coding, errors in movement endpoints, i.e. target specific error distributions, should result from errors that depend on the hand displacement vector. Thus, endpoint errors that result from random combination of observed displacements and observed start points should be the same as endpoint errors that we observe in our data. To test if this is the case, we computed SD_{2D} of fictional endpoints in a next step (Fig. 4f) and then compared the magnitude of fictional and observed endpoint SD_{2D} by taking the ratio of observed over fictional endpoint SD_{2D}. This ratio can be interpreted as the proportion of the variance that can be explained based on vector coding, i.e. hand-centered control. If we multiply it by 100, we obtain a percentage. If the CNS uses hand-centered control, i.e. vector coding, the proportion of variance that can be explained should be close to 100%. A similar analysis was performed for "Displacement" conditions, with the difference, that we first aligned movements on those targets that had been used as starting point in the computation of the target displacement to remove instruction based movement shifts. After alignment, we can then compute observed and fictional displacements in the same way as in "Endpoint" conditions.

To determine to what degree subjects use target centered control, i.e. endpoint coding, in "Endpoint" conditions, we followed the steps illustrated in Fig. 4g–k. First, we computed all observed displacements made from any other target towards a certain main target (Fig. 4g). We then aligned the displacements at their origin and computed the SD_{2D} of the aligned observed displacements by fitting a minimum variance ellipse. This is equivalent to computing movement errors that depend on the hand displacement vector (Fig. 4h). In a next step, we combined observed endpoints with observed start points from other movements that had been made to the same target. This is equivalent to reshuffling target specific errors (Fig. 4i). From this recombination, we obtained fictional displacements (Fig. 4j). If subjects use target centered control, i.e. endpoint coding, errors in hand displacements, should result from errors that depend on targets in space. Thus, displacements that result from recombination of start and endpoints should be the same as the ones that we observe in our data. To test if this is the case, we aligned the fictional displacements and computed their SD_{2D} (Fig. 4k) and then compared the magnitude of fictional and observed displacement SD_{2D} by taking the ratio of observed over fictional displacement SD_{2D}. This ratio can be interpreted as the proportion of the variance that can be explained by target centered control, i.e. endpoint coding. If we multiply it by 100, we obtain a percentage. If the CNS uses
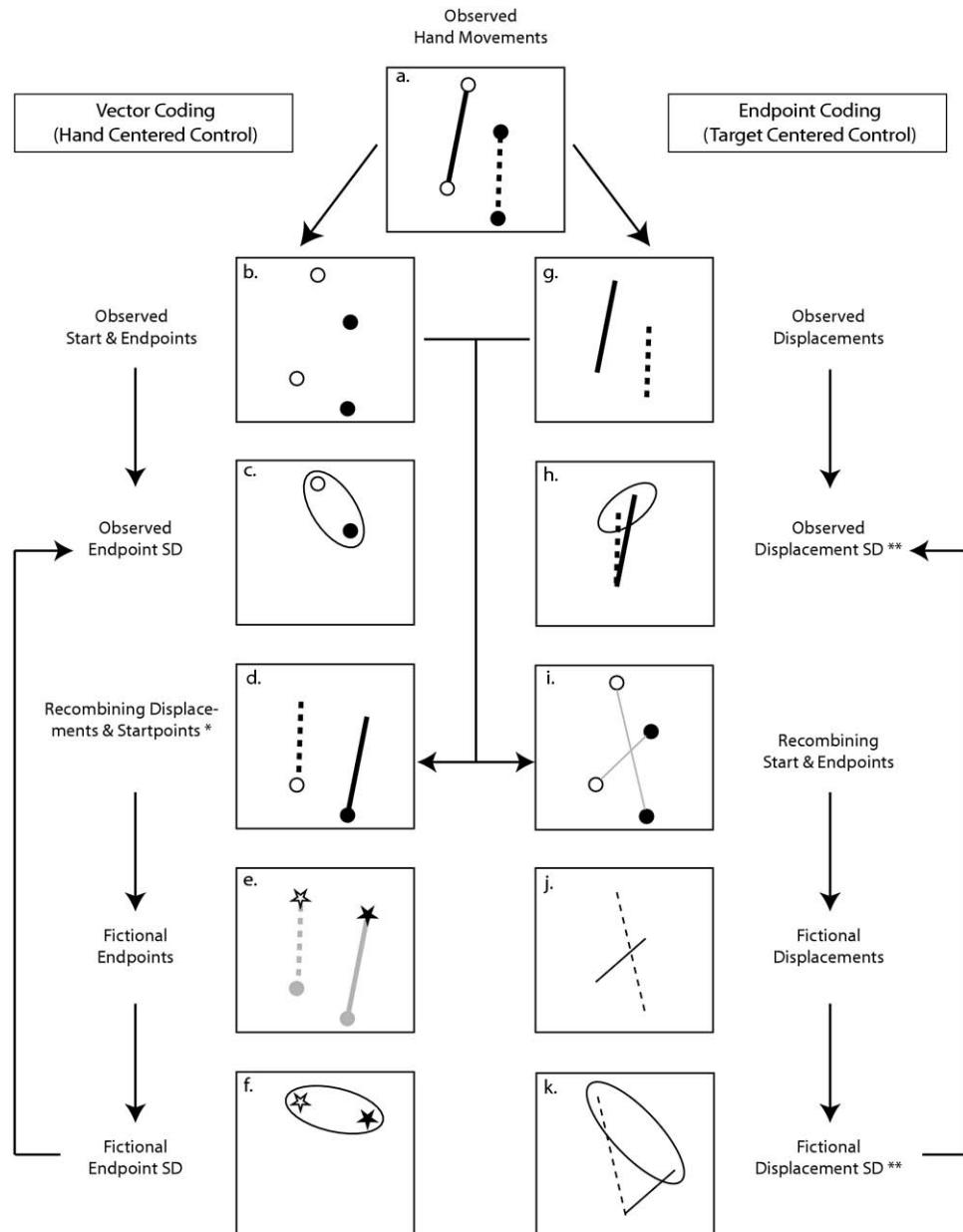
Fig. 4. Illustration of control system analysis. * Displacements were transformed into displacement errors before recombination (see Appendix A). ** Displacements were normalized before computation of SD_{2D} (see Appendix B).

target-centered control, i.e. endpoint coding, the proportion of variance that can be explained should be close to 100%. A similar analysis was performed for "Displacement" conditions with the difference that we first aligned movements on those targets that had been used as starting point in the computation of the target displacement to remove instruction based movement shifts. After alignment, we can then compute observed and fictional displacements in the same way as in "Endpoint" conditions.

The analysis described in the previous paragraph and illustrated in Fig. 4g–k is biased towards endpoint coding, whenever spatial variability introduced by experimental layout is large compared to spatial variability introduced by central visuo-motor processes. To improve the sensitivity of our analysis we thus normalized observed and fictional displacements prior to computing their SD_{2D}. Please see Appendix B for a detailed explanation and computational details.

To create fictional endpoints or displacements we recombine movement components from different trials and due to pseudo-randomization, we can recombine movement components that occurred within an average separation of multiples of six trials. Systematic variation of the number of intervening trials allows us to determine if there are systematic shifts in performance over time. If there is a systematic shift, we should see a systematic change in computed ratios as the number of intervening trials increases (van den Dobbelsteen et al., 2001).

Model simulations

In an effort to confirm the validity of the control parameter analysis and to assess how it would be affected by central and peripheral noise, we simulated the performance of ideal subjects using dif-

ferent control schemes and analyzed the results using the same analyses that were applied to the actual subjects. We simulated subjects using hand- and target-centered control in the presence of different levels of peripheral noise (0%–100% peripheral noise in 10% steps). At 0% peripheral noise, all movement errors are determined by noise that arises in the determination of the goal state of the hand. At 100% percent peripheral noise, all movement errors are determined by noise that arises at the neuromuscular junction during movement execution. Assuming independence between central and peripheral noise (van Beers et al., 2004) errors from the two processes were added. However, please note that even though peripheral and central errors are statistically independent and thus added, the distribution of peripheral noise is nevertheless contingent on central noise, because the planned goal state of the hand determines movement magnitude and direction and thus distribution characteristics of peripheral noise.

We simulated five different aspect ratios (major/minor axis) of central visuo-motor error ellipses (2.5, 2, 1.7, 1.3 and 1) as well as three different total noise levels (7.5%, 10% and 15%). Both vector and endpoint coding models were simulated 100 times at all levels of execution noise, yielding 1100 simulated data sets for each model and central noise aspect ratio. Each simulation "performed" the same experiment as any of our subjects and thus gave a total of 2 (conditions)×6 (blocks)×49 (trials)=588 responses and 12 responses to each path between any two main coordinates of a configuration in both "Displacement" and "Endpoint" conditions. The following paragraphs briefly describe the gist of our simulations. A more detailed description is given in Appendix C.

Peripheral noise was modeled as noise in the results as zero-mean, bivariate gaussian errors, or error ellipses, respectively, based on the execution noise distribution characteristics reported by van Beers et al. (2004). We implemented peripheral noise in the results, instead of process noise, because result noise is sufficient to investigate its effect on our analysis.

Central, vector coding noise was modeled as normally distributed with standard deviations proportional to the amplitude of the hand-target vector (Gordon et al., 1994; Messier and Kalaska, 1997). In "Endpoint" conditions, the hand target vector was obtained by computing the vector pointing from the current simulated hand position towards the visible target. In "Displacement" conditions, the hand target vector was equal to the visual displacement vector. To obtain error ellipses that are elongated in the direction of the hand-target vector, standard deviation of errors orthogonal to the hand-target vector was chosen to be a scaled version of standard deviation of errors along the hand-target vector. Choosing error distributions this way, results in bivariate gaussian error distributions, i.e. central noise error ellipses, whose aspect ratio is constant across movement direction and whose area increases with increasing hand-target vector amplitude. Assuming zero mean noise, central error ellipses are positioned on the (either visible or virtual) target.

Central, endpoint coding noise was modeled in the same way as hand-centered noise, with the only difference that errors were computed with respect to eye/head-target vector, instead of hand-target vector (McIntyre et al., 1997, 1998; Carrozzo et al., 1999; van den Dobbelsteen et al., 2001). For our model, we assume that subjects compute target coordinates either with respect to the line of sight (in eye-centered coordinates) or with respect to the line passing from the stationary cyclopean eye through the visible or virtual target (head centered). It follows that eye- and head-centered models are equivalent in our experiment. Thus, in "Endpoint" conditions we obtained the eye/head—target vector by computing the vector pointing from the cyclopean eye towards the visible target. In "Displacement" conditions, it was obtained by shifting the visual displacement vector onto the current simulated hand position and computing the vector pointing from the cyclopean eye towards the endpoint of the shifted displacement vector. Since subjects did not receive feedback on their current hand position in

Table 1. Statistics on various movement parameters computed across movement paths, configurations and subjects

	Mean	SD	Median	Min	Max
Endpoint conditions					
Mean velocity (cm/s)	10.5	1.9	10.2	6.8	16.4
Peak velocity (cm/s)	37.1	8.5	34.9	23.9	62
Duration (s)	1.2	0.2	1.2	0.7	1.5
Curvedness (%)	4.3*	2.9	3.5	1.3	16.9
Movement amplitude (mm)	119	26	115.0	76	197
Displacement conditions					
Mean velocity (cm/s)	10.5	1.9	10.4	5.8	16.1
Peak velocity (cm/s)	36.1	7.4	35.2	20.9	60.7
Duration (s)	1.1	0.2	1.1	0.8	1.6
Curvedness (%)	2.5	0.7	2.4	1.2	4
Movement amplitude (mm)	113	23	112.0	65	166

* Significant difference in means between "Endpoint" and "Displacement" conditions, $P<0.05$.

"Displacement" conditions, we assumed for this simulation that subjects estimated current hand position proprioceptively.

RESULTS

Behavioral results

Movement kinematics and trajectory shape. Table 1 shows the results of the analysis of movement velocities, duration, distance and curvedness across configurations and spatial coordinates and subjects. To assess statistical significance we applied a repeated measures ANOVA with "condition" and "path" as repeated measures factors, where "path" was defined as the 12 distinct paths between any two main coordinates across both configurations. Except for trajectory curvedness, none of these measures exhibited a significant main effect of "condition" or a significant interaction. Movement trajectories are significantly more curved in "Endpoint" than in "Displacement" conditions ($F_{1,7}=7.689$, $P=0.028$), as indicated by a 1.8% drop in curvedness from 4.3% in "Endpoint" conditions to 2.5% in "Displacement" conditions. However, curvedness values are overall very low indicating that movement trajectories were very close to straight-line trajectories in both conditions. In summary, it appears that physical movement parameters do not differ between "Endpoint" and "Displacement" conditions. Since peripheral noise depends on physical movement parameters such as movement velocity, duration, distance and trajectory shape we can assume that peripheral noise does not differ between "Endpoint" and "Displacement" conditions.

Error distributions. Fig. 5 shows ellipses fitted to distributions of endpoints in "Endpoint" and "Displacement" conditions. For better visibility, the length of each axis in Fig. 5 corresponds to four times the standard deviation along that axis. Ellipses obtained for clockwise and counterclockwise movement directions have been plotted with solid and dashed lines, respectively. To allow for easy visual comparison of ellipse size and shape, ellipses are
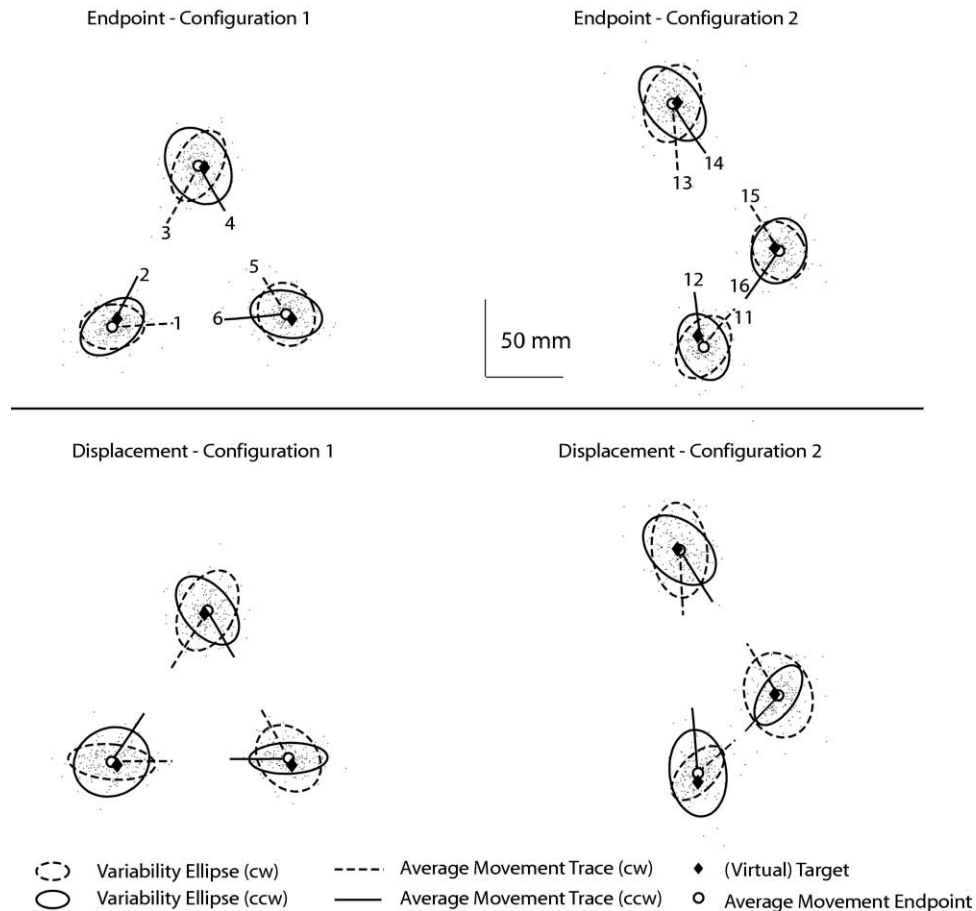
Fig. 5. Distributions of movement endpoints in "Endpoint" and "Displacement" conditions for each path between main targets in a configuration. Ellipse axes denote four standard deviations around the mean. Ellipses were computed for each path after subtracting each subjects mean for that path. For easier visual comparison, individual subject's movement endpoints and ellipses are aligned on the group mean for a (virtual) target. Parts of average movement traces have been plotted to indicate alignment with the last part of a movement trajectory. Numbers identify ellipses and their corresponding paths.

positioned on the average movement endpoint across subjects and paths for a given target. To provide visual indicators of ellipse alignment with the last part of a movement trajectory, the last part of average movement trajectories along each path has been plotted as well. Numbers identify ellipses and their corresponding paths.

Overall, it is apparent from Fig. 5 that distributions of endpoints vary in size, shape and orientation depending on the movement path. Ellipses are generally elongated in the direction of movement and aligned with the last part of the movement trajectory, indicating that movement variability depends on the direction of movement in hand centered coordinates. Comparing corresponding ellipses between "Endpoint" and "Displacement" conditions reveals that even though some ellipses show a tendency to be more elongated in the direction of movement in "Displacement" conditions (i.e. ellipses 1, 6, 11 and 16) differences are rather subtle. Furthermore, some ellipses do not appear to differ in elongation at all (i.e. ellipses 3, 4, 13, 14 and 15) and some are actually less elongated in "Displacement" compared to "Endpoint" conditions (ellipse 2). Overall, the size of ellipses, i.e. overall error magnitude, appears to be

similar across the two conditions, even though one ellipse (ellipse 15) increases noticeable in size in "Displacement" conditions.

To determine if there are statistically significant differences in ellipse shape between "Endpoint" and "Displacement" conditions, we applied repeated measures ANOVA with "condition" and "path" as repeated measures factors to each of the various ellipse shape measures shown in Table 2. The "path" factor was defined as the 12 distinct paths between any two main coordinates across both configurations. None of the analyses revealed a significant main effect of condition. This result is in agreement with our observation from Fig. 5 that on a global level ellipse shape and size does not seem to differ between "Endpoint" and "Displacement" conditions. However, all analyses revealed a significant interaction between "condition" and "path." This result is in agreement with our observation from Fig. 5 that some ellipses change shape, even though the change may go into different directions (i.e. increase or decrease in elongation) for different ellipses. To determine for which ellipses changes in shape are statistically significant we computed paired samples t-test for each shape

Table 2. Various measures of ellipse shape

Statistic	Endpoint conditions		Displacement conditions		Ellipses that are significantly different ($P<0.05$)
	Average	SD	Average	SD	
On axis error (mm)	10.5	4.70	12.5	3.4	1, 15
Off axis error (mm)	7.7	3.20	7.9	2.8	15
ON/OFF	1.45	0.63	1.8	0.99	1, 6
Major axis length (mm)	11.4	5.00	13.1	3.2	1, 15
Minor axis length (mm)	6.4	2.30	7.0	2.4	2, 12, 15, 16
Major/minor	1.83	0.68	2.1	1.1	1
SD_{2D} (mm^2)	64	47.00	75	37	15

Averages and SD were computed across configurations, paths and subjects. Significance was assessed using paired samples t-tests. Ellipse numbers correspond to ellipse numbers in Fig. 5.

measure between corresponding ellipses in "Endpoint" and "Displacement" conditions. The results of this analysis are shown in Table 2. The results are in good agreement with Fig. 5, in that ellipses that are statistically significantly different also look different (ellipses 1, 2, 6, 16 and 15).

In summary, ellipse shape appears to depend on the movement path, i.e. distance and direction in hand-centered coordinates, in both conditions. Even though there are some statistically significant differences in ellipse shape between "Endpoint" and "Displacement" conditions, our statistical analysis indicates that these differences are limited to certain movement paths and do not apply on a global level. Furthermore, changes are not consistent for the two conditions, i.e. some ellipses increase in elongation, whereas others decrease. Most importantly, overall SD_{2D} and thus overall error magnitude is the same in "Endpoint" and "Displacement" conditions.

Based on this traditional analysis of movement endpoint distributions there appears to be no difference in distributions of movement endpoints, and thus no difference in the coordinate system that the CNS uses for movement planning in "Endpoint" and "Displacement" conditions. Furthermore, the observation that ellipses are generally aligned with the direction of movement is consistent with previous reports in the literature that investigated hand movements in the plane (Messier and Kalaska, 1997) and one might conclude that subjects use hand-centered control, i.e. vector coding, in both tasks in our experiment. However, as mentioned in the introduction, an interpretation of distributions of movement endpoints solely in terms of central visuo-motor processes is problematic (Churchland et al., 2006) and the alignment of movement endpoints with the direction of movement could also be explained based on peripheral noise (van Beers et al., 2004).

Constant movement errors. Fig. 6 shows each subject's average movement endpoint for a given path. Averages were computed for movement paths between any two main targets in a configuration. Group averages in clockwise and counterclockwise movement directions have been connected with solid and dashed lines, respectively. It is apparent that movement endpoints in "Endpoint" and "Displacement" conditions are virtually identical. It is also evident that despite individual differences average endpoints of subjects' movements are shifted in the direc-

tion of movement in clockwise and counterclockwise directions, respectively. The average spatial shift of endpoints with respect to each other is 8.4 mm. Overall, it is evident from the average movement endpoints that subjects are equally accurate in both "Endpoint" and "Displacement" conditions. Average movement endpoints therefore do not differ between the two conditions and one might conclude that subjects rely on the same central visuomotor processes in "Endpoint" and "Displacement" conditions.

Control system analysis. Our control system analysis is a potentially more powerful tool to investigate how movements are controlled. As mentioned in the introduction the analysis used in the current paper is an extension of an analysis first introduced by van den Dobbelsteen et al. (2001). Fig. 7 shows the results of our analysis for both "Endpoint" and "Displacement" conditions. Filled and open symbols indicate average percentage of variance accounted for by endpoint coding (target centered control) and vector coding (hand centered control), respectively, across subjects, targets and configurations. Denoted on the abscissa is the average number of movements that separated movements used for recombination. Dotted lines indicate the beginning of a new block. Since presentation order of the two different target configurations was pseudo-randomized within "Displacement" and "Endpoint" sessions, each dotted line corresponds to an average gap of one block of (49 movements). Error bars indicate standard errors of the mean across subjects, targets and configurations.

It is apparent from Fig. 7 that in "Endpoint" conditions endpoint coding accounts for a larger proportion of movement variance (75%) than vector coding (60%). The opposite pattern of results holds in "Displacement" conditions, where vector coding accounts for a larger proportion of movement variance (90%) than endpoint coding (65%). This finding is strong evidence for the idea that central visuo-motor processes differ between "Endpoint" and "Displacement" conditions. Specifically, our results suggest that subjects employ hand-centered control in "Displacement" conditions, and target-centered control in "Endpoint" conditions. Interestingly, our analysis reveals this difference between "Endpoint" and "Displacement" conditions, even though standard analyses of distributions of movement endpoints do not.
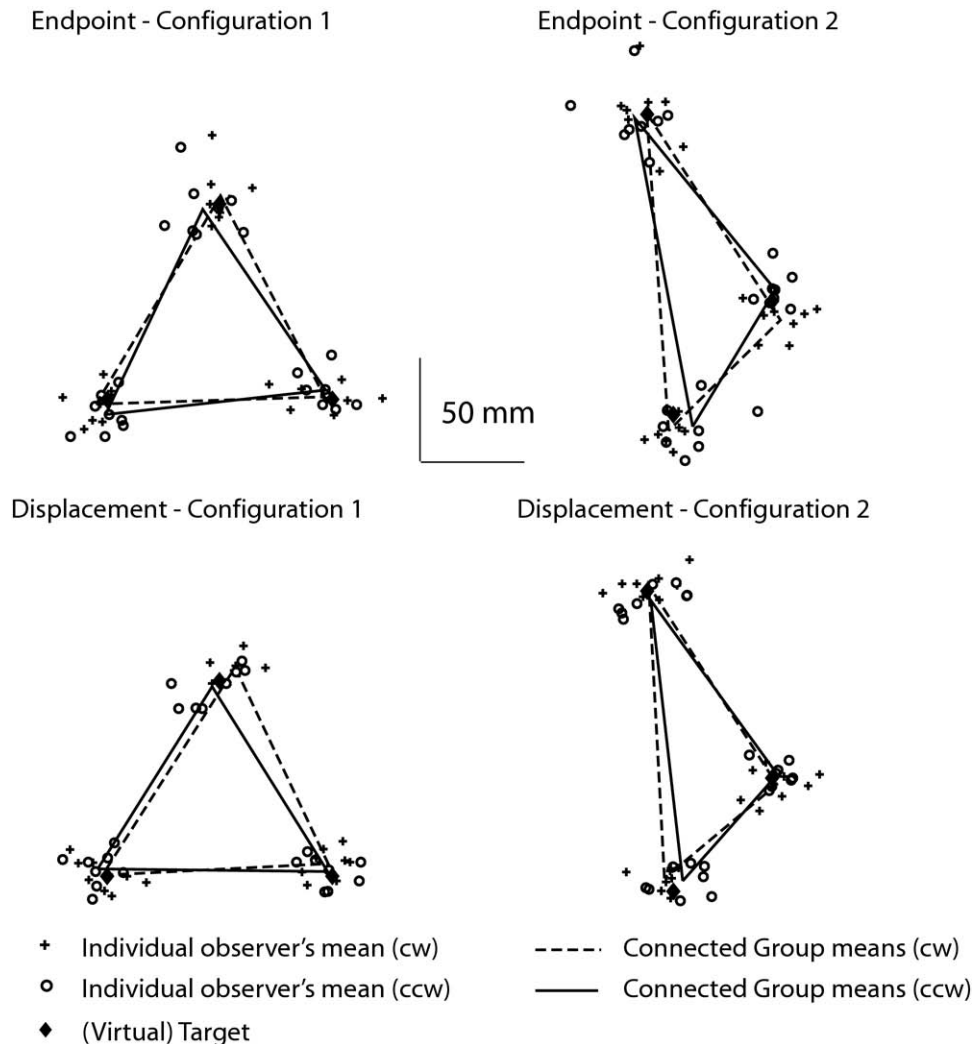
Fig. 6. Average movement endpoints in "Endpoint" and "Displacement" conditions computed for every path between main targets in a configuration. Group means have been connected with lines to show systematic shifts.

In "Endpoint" conditions, there is a small systematic change in observed ratios over time. However, a repeated measures ANOVA with "average shift" as repeated measures variable revealed that neither linear nor quadratic trends are significant. Thus, we conclude that there is no systematic shift in hand position over time in our data.

The results obtained on the group level hold for individual subjects as well. To obtain a compact measure of performance for each subject we computed the normalized difference d in explained variability between hand- and target-centered control for "Endpoint" and "Displacement" conditions as $d = (\bar{P}_{target} - \bar{P}_{hand}) / \sqrt{(s^2_{target} + s^2_{hand})/2}$, where $\bar{P}$ is the average proportion of explained variability and s^2 is the sample variance across targets, configurations and movement shifts. d is negative when hand-centered control, i.e. vector coding, explains a higher proportion of variability and positive when target-centered control, i.e. endpoint coding, explains a higher proportion of variability. Fig. 8 shows d plotted separately for "Endpoint" and "Displacement" conditions. As expected, d is positive (mean=1.2)

for all subjects in "Endpoint" conditions and negative (mean=-1.1) for all subjects in "Displacement" conditions and the difference is significant ($t_{(7)}=4.79$, $P=0.002$, t-test for paired samples, two-tailed). We did not find systematic differences between targets.

Simulation results

Validity of control system analysis. To confirm the validity of our analysis we simulated the performance of ideal subjects using endpoint and vector coding in the presence of different levels of peripheral noise. We then applied the control system analysis to each simulated data set in the same way that we analyzed the movement data of the actual subjects to determine the normalized difference d in the proportion of explained variability between target- and hand-centered control for each simulation. It is important to keep in mind that d is negative when hand-centered control explains a higher proportion of variability and positive if target-centered control explains a higher proportion of variability. Thus, if this is indeed a valid
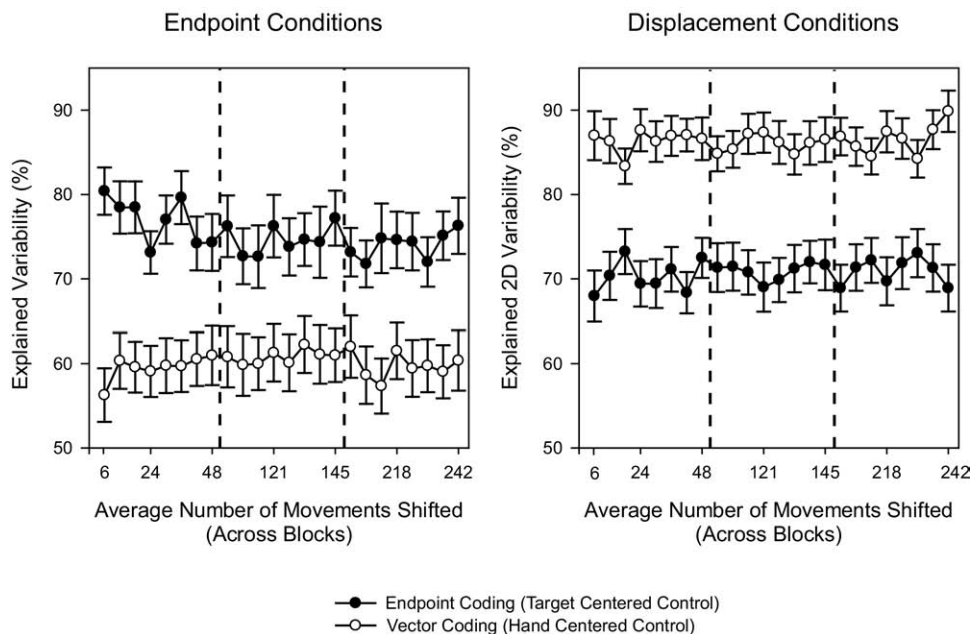
Endpoint Conditions

Displacement Conditions

Fig. 7. Results of the control system analysis in "Endpoint" and "Displacement" conditions. Denoted on the ordinate is the average percentage of variance accounted for by endpoint and vector coding, i.e. target- and hand-centered control, respectively, across subjects, targets and configurations. Denoted on the abscissa is the average number of movements that separated movements used for recombination. Dotted lines indicate the beginning of a new block (gap of 49 movements). Error bars indicate standard errors of the mean across subjects, targets and configurations.

analysis, then d should be positive when a data set is generated by the endpoint coding model, and it should be negative when a data set is generated by the vector coding model. For each condition, we also computed the probability that our analysis correctly recovers the model that generated the data $p(m|m)$.

We found that d and $p(m|m)$ were unaffected by aspect ratio of central noise as well by absolute level of noise. Therefore, Fig. 9 shows d collapsed across aspect ratios of central noise and total noise levels and plotted as a function of peripheral noise level. The left and right panels show the results in "Endpoint" and "Displacement" conditions, respectively, and filled and open symbols repre-

Fig. 8. Normalized difference in proportion of explained variability between hand- and target-centered control (D) in "Endpoint" and "Displacement" conditions.

sent average d for data sets generated by endpoint coding and vector coding models. Numbers above each data point indicate $p(m|m)$ across aspect ratios of planning noise and total noise levels. Error bars denote standard deviation of d.

It is evident from Fig. 9 that d and $p(m|m)$ are systematically affected by levels of peripheral noise. In both "Endpoint" and "Displacement" conditions, d is well above zero for data sets generated by the endpoint coding model and well below zero for data generated by the vector coding model when peripheral noise level is zero and $p(m|m)$ is one or close to one. This indicates that our control system analysis correctly recovers the model that generated the data when no peripheral noise is present. However, as peripheral noise increases, d as well as $p(m|m)$ decreases for data sets generated by the endpoint coding model. In "Endpoint" conditions, d is well above zero and $p(m|m)$ is larger then 0.9 until peripheral noise level reaches 60%. In "Displacement" conditions, d is well above zero and $p(m|m)$ is larger than 0.9 only until peripheral noise level reaches 30%. Thus, when peripheral noise exceeds 60% in "Endpoint" conditions and 30% in "Displacement" conditions, our coordinate system analysis has a bias to attribute higher proportion of explained variability to the vector coding model, even though the data set was actually created by the endpoint coding model. The bias is stronger in "Displacement" conditions. In summary, the results suggest that our analysis will reliably identify an endpoint coding model, when peripheral noise is less than or equal to 60% in "Endpoint" conditions and less than or equal to 30% in "Displacement" conditions. Otherwise, peripheral noise mimics vector coding in our analysis. This is ex-
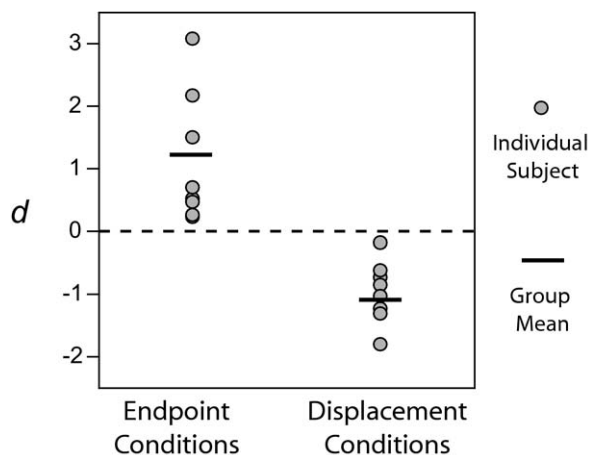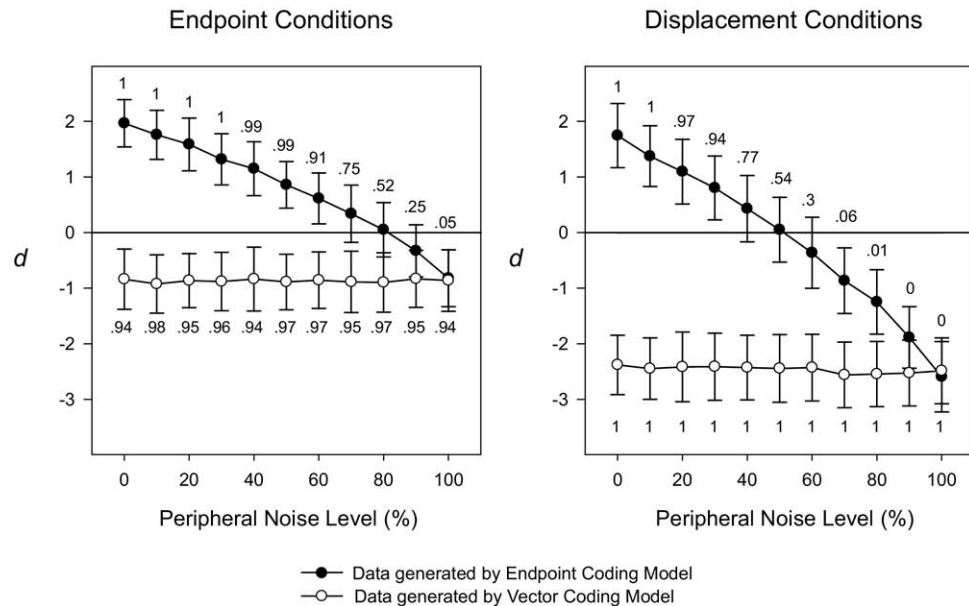
Fig. 9. Normalized difference in proportion of explained variability between hand- and target-centered control (D) for data generated by the vector coding model (open symbols) and endpoint coding model (filled symbols) in "Endpoint" and "Displacement" conditions plotted as a function of peripheral noise level. Numbers above each data point represent the probability to correctly recover the model p(m|m) that generated the data. Average d and p(m|m) was computed across noise aspect ratios and absolute noise levels. Error bars denote standard deviations.

pected, since the movements that we simulated were similar to the visual hand-target vector.

Given the fact that peripheral noise mimics central noise stemming from vector coding processes in our analysis, it follows that the average normalized difference d and recovery probability p(m|m) of target-centered control in "Endpoint" conditions can serve as indicators of the degree of peripheral noise present in the data, i.e. if d is around 1 and we recover endpoint coding 100% of the time in "Endpoint" conditions, the level of peripheral noise is expected to be between 40% and 50%. In contrast, if we recovered vector coding 75% of the time in "Endpoint" conditions, this could indicate either hand-centered control or that peripheral noise level is 90%.

In the analysis of our subjects' data, endpoint coding won all samples in "Endpoint" conditions, and average d is 1.2 (compare Fig. 8). Based on this we can assume that peripheral noise is around 40% in our experiment. Furthermore, given the high similarity of movement velocity and duration between "Endpoint" and "Displacement" conditions, we can also assume that peripheral noise is comparable across the two tasks. We conclude that our analysis is a valid indicator of visually induced differences in the way movements are controlled in our experiment.

Estimate of peripheral noise in our data. As stated in the previous paragraph, endpoint coding won all samples in "Endpoint" conditions and average d is 1.2. Furthermore, movement velocity, duration, distance, etc. are very similar in "Endpoint" and "Displacement" conditions, such that peripheral noise can be assumed to be constant. Based on these observations we could estimate the peripheral noise level in our data to be approximately 40%. An estimate of 40% would be similar to a recent estimate derived from

neuronal activity in dorsal premotor and primary motor cortex (Churchland et al., 2006). In their experiment, Churchland et al. (2006) measured movement speed and found that neuronal activity prior to movement onset predicts 50% of the observed variability in movement speed, suggesting that the remaining 50% are due to peripheral noise arising during movement execution. Churchland et al.'s (2006) task was highly repetitive. In contrast, our task required the planning of new movement parameters on every trial. If we assume that the estimate of 40% is a correct estimate of peripheral noise level in our data, we are therefore led to the conclusion that even for non-repetitive tasks the contribution of peripheral noise can be as high as 40%.

The analysis described above is based on the implicit assumption that subjects use either pure endpoint coding or pure vector coding. However, another possible interpretation of our results is that the CNS uses a combination of endpoint and vector coding to guide the hand (Abrams et al., 1990; De Grave et al., 2004), and in that case the amount of peripheral noise needed to explain our data would be less than 40%. Based on the idea of a hybrid-control system, differences between "Endpoint" and "Displacement" conditions would be caused by differences in the relative contribution of endpoint and vector coding in the two tasks. Since peripheral noise mimics the use of hand-centered control in our experiment, it is impossible to distinguish the use of vector coding from the presence of peripheral noise. However, there are two reasons why we think that it is likely that subjects use combination of target- and hand-centered control in our experiment. First, it has been shown that when subjects move towards a visible target the perception of length in hand centered coordinates contributes approximately 8% to overall movement

amplitude (De Grave et al., 2004). This finding suggests that vector coding might contribute approximately 10% to overall movement variability in our "Endpoint" task, and that the level of peripheral noise might be approximately 30%. Second, the *d*-value of −1.1 in displacement conditions in our experiment is highly indicative of a combined use of endpoint and vector coding, because that value would only be expected if 30% of the variability in "Displacement" conditions is due to endpoint coding (see Fig. 9). Thus, for both "Endpoint" and "Displacement" conditions there is good reason to suspect that subjects use a combination of target- and hand-centered control, but that the relative contribution of either process differs between the two tasks.

In summary, we cannot give an exact estimate of peripheral noise in our data, because peripheral noise mimics the use of hand-centered control in our experiment. Based on other reports in the literature, however, an estimate between 30% and 40% appears reasonable.

Explaining error distributions (Fig. 5) based on our control system analysis (Figs. 7 and 8)

In light of these conclusions, it is useful to reconsider our finding that distributions of movement endpoints are aligned with the direction of movement in both "Endpoint" and "Displacement" conditions (Fig. 5). The alignment of movement endpoint distributions in "Displacement" conditions is expected, since our control system analysis reveals that subjects use vector coding in these conditions (Figs. 7 and 8). However, the alignment in "Endpoint" conditions is unexpected because our control system analysis suggests that subjects use endpoint coding in these conditions (Figs. 7 and 8). In fact, based on endpoint coding we would expect that distributions of movement endpoints towards the same target overlap perfectly and that there should be no systematic alignment with movement direction.

Fortunately, we can reconcile these seemingly inconsistent results based on the finding that only 60% of movement variability in "Endpoint" conditions is due to target centered control, and therefore, that the remaining 40% are due to either peripheral noise and/or hand centered control. Since both processes will result in endpoint errors that depend on the visual hand-target vector in our experiment, their contribution to overall movement variability in "Endpoint" conditions will align movement endpoint distributions in "Endpoint" conditions with the direction of movement.

To test if this explanation is borne out in practice we ran simulations for both "Endpoint" and "Displacement" conditions. Based on a suggestion by an anonymous reviewer, we used our empirically observed values of *d* (Fig. 8) to select relative contributions of target-, hand-centered and peripheral noise for our simulations. Since *d* was 1.2 in "Endpoint" conditions, the contribution of endpoint coding to movement variability in "Endpoint" conditions was chosen to be 60%. The remaining 40% in "Endpoint" conditions was chosen to consist of 30% peripheral noise and 10% vector coding. In "Displacement" conditions, model

parameters were chosen based on the following reasoning. First, peripheral noise level in "Displacement" conditions has to be the same as in "Endpoint" conditions, i.e. 30%. Second, we observed an average *d* of −1.1 in "Displacement" conditions, which implies that endpoint coding contributes ~30% to overall movement variability. Choosing 30% endpoint coding noise and 30% peripheral noise leaves a remainder of 40% movement variability that must be due to vector coding in "Displacement" conditions. To summarize, for "Displacement" conditions the contribution of endpoint coding, vector coding and peripheral noise to movement variability was chosen to be 30%, 40% and 30%, respectively.

For simulations in both "Endpoint" and "Displacement" conditions, we used noise characteristics described in Appendix C. We deliberately chose the aspect ratio of central noise error distributions to be 1.7 and total noise level to be 15%. We simulated 100 data sets for each condition. We then analyzed distributions of simulated movement endpoints in the same way as we had analyzed our subjects' data (see Experimental Procedures: "Analysis of Distributions of Movement Endpoints").

Fig. 10 shows simulated distributions of movement endpoints for "Endpoint" and "Displacement" conditions plotted in the same format as our empirically observed data in Fig. 5. The only difference between Figs. 5 and 10 is that Fig. 5 shows portions of average movement traces to illustrate alignment with direction of movement, whereas Fig. 10 shows portions of the visual hand-target vector instead. Choosing aspect ratios smaller or larger than 1.7 for the simulations will result in ellipses that are overall less or more elongated, while leaving variations in aspect ratio between paths, configurations and conditions unaffected. Choosing different total noise levels will result in scaled versions of the same ellipses.

It is evident from Fig. 10 that simulated ellipses align with the direction of movement in all conditions. Furthermore, it is also evident that there are differences in ellipse shape between different movement paths and between "Endpoint" and "Displacement" conditions, i.e. ellipses are more or less elongated or larger and smaller for certain paths. To determine quantitatively how the simulated data capture variations in endpoint distributions generated by our subjects we computed major and minor axis lengths of corresponding ellipses shown in Fig. 10 and Fig. 5. We then correlated corresponding axes lengths separately for major and minor axes and for major and minor axes combined. We also computed the orientation of ellipses by computing major axis orientation. We limited major axis orientation to the range 0–179°, since left/right up/down pointing ellipses are the same. To determine quantitatively how similar major axis orientation is between subject generated and simulated data, we computed the angular-angular correlation between corresponding major axes orientations (Fisher, 1993). Figure 11 shows plots of ellipse axes orientation and length in the left and right panel, respectively. Correlation coefficients are indicated in each plot.
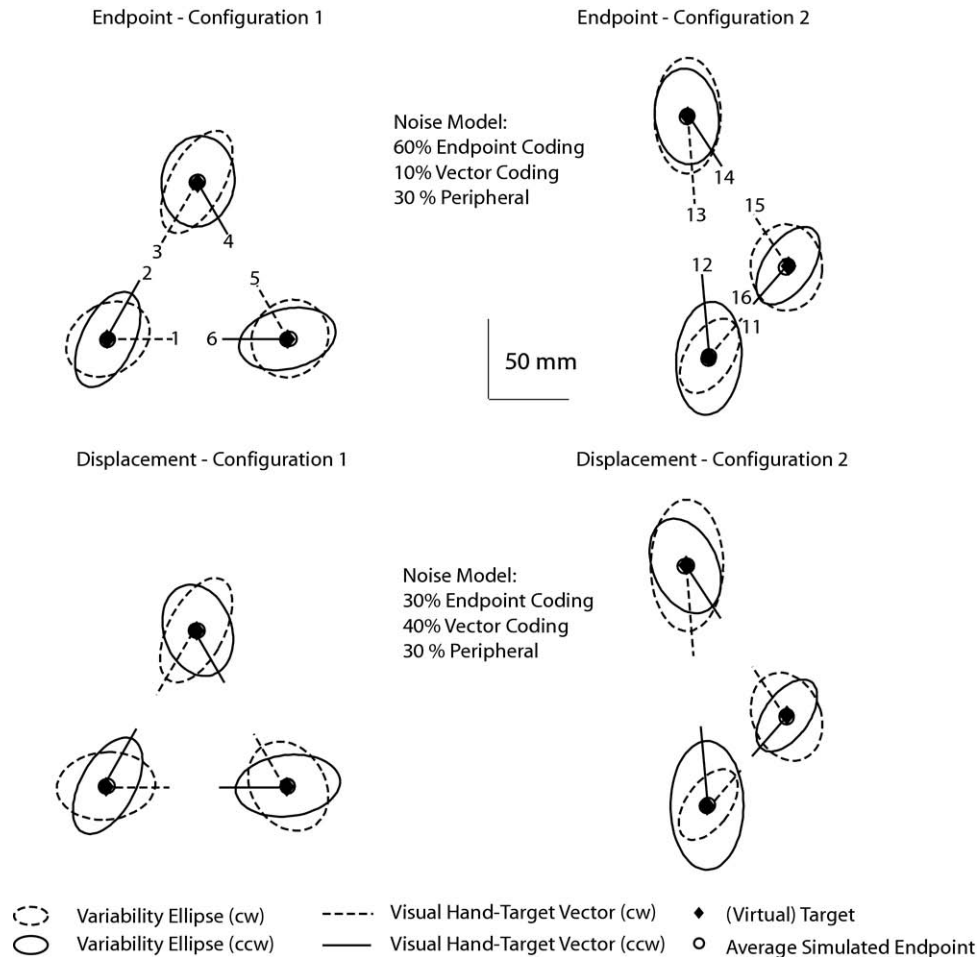
Fig. 10. Distributions of simulated movement endpoints in "Endpoint" and "Displacement" conditions for each path between main targets in a configuration. Ellipse axes denote four standard deviations around the mean. For easier visual comparison, ellipses are aligned on the group mean for a (virtual) target. Parts of the visual hand-target vector have been plotted to indicate ellipse alignment with the simulated direction of movement. Numbers identify ellipses and their corresponding paths and correspond to numbers in Fig. 5.

It is evident from the left panel in Fig. 11 and the high angular-angular correlation ($r=0.86$, $z=3.31$, $P<0.001$) that ellipse orientation between subject-generated and -simulated data correspond well. For ellipse axis length, we observe that axes of simulated data generally exceed those of subject-generated data, because we arbitrarily chose 15% overall noise level. Since overall noise level is a scale parameter it does not affect variation in ellipse axes length, however. With regard to variations in ellipse axes length, observe that our model predicts differences between major and minor axes lengths well. This is indicated by the comparably low scatter in Fig. 11 (right panel) and the high correlation coefficient when it is computed for minor and major axes combined ($r=0.86$, $t_{(46)}=11.4$, $P<0.0001$). Correlations drop when we correlate simulated and subject generated axis length separately for minor and major axes (major axes: $r=0.61$, $t_{(22)}=3.6$, $P<0.005$) minor axes: $r=0.52$; $t_{(22)}=2.86$, $P<0.01$). This indicates that our model simulations predict variation between major and minor axes lengths better than variations within minor and major axis lengths.

We discovered that we could make the simulated data predict our subjects' data better by changing peripheral noise characteristics, such as the direction in which execution noise ellipses are maximally elongated (compare Fig. A in Appendix C). Even though van Beers et al. (2004) report that execution noise is affected by location of workspace and subjects specific differences, we do not have a principled way to determine those parameters for our current data. Thus, even though it is possible to create a better fit between simulated and observed data, Figs. 10 and 11 only show the results based on general execution noise characteristics reported by van Beers et al. (2004).

In conclusion, our analyses suggest that ellipses derived from our simulated data correspond reasonably well to ellipses derived from subject-generated data. Thus, even though the results in Fig. 5 and Figs. 7 and 8 appear contradictory at a first glance, they are not. In fact, simulations that incorporate both central and peripheral noise sources can account for various aspects of our data. This finding further emphasizes that distributions of movement endpoints are affected by both central and peripheral noise
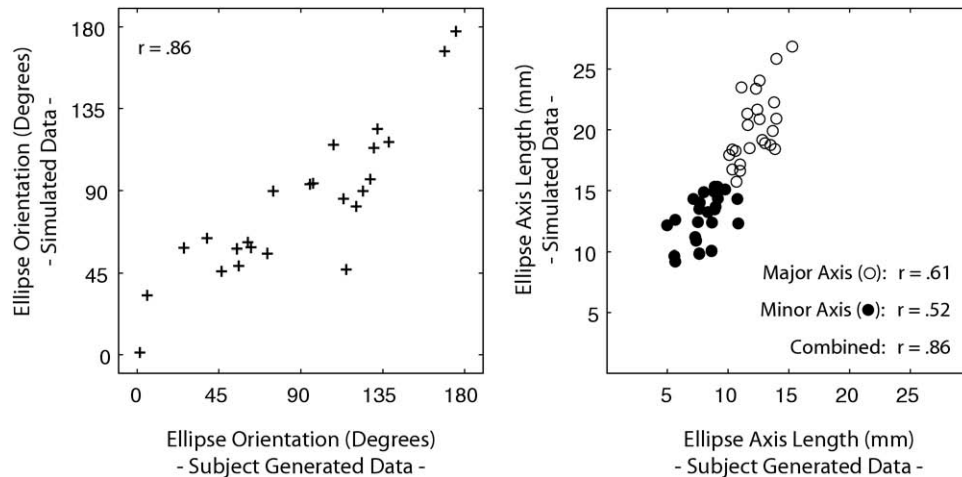
Fig. 11. Scatter plots of ellipse parameters derived from subject generated and simulated data, i.e. parameters of ellipses shown in Fig. 5 and Fig. 10, respectively. Ellipse orientations are plotted on the left. Ellipse major and minor axes are plotted on the right. Please note that orientations of both 0 and 180° denote ellipses whose major axes are oriented horizontally.

processes and that this has to be considered in their interpretation.

DISCUSSION

One of the major research questions regarding central visuo-motor processes regards the question which parameters the CNS controls to guide the hand. In the literature, models that use hand- and target-centered control are referred to as vector and endpoint coding models, respectively. Here we used a sequential movement paradigm that manipulated the way visual information relevant for movement production was presented to investigate if the CNS is flexible in its choice of control parameters. We analyzed spatial movement errors using a traditional analysis of movement endpoint distributions and a new analysis that uses different recombination rules to investigate the contribution of endpoint and vector coding to movement control. We used simulations to test if our new analysis recovers the control model that generated the data under different levels of peripheral noise.

Our control system analysis reveals that subjects employ target centered control, i.e. endpoint coding, when they can reach towards a visible target but that they use hand-centered control, i.e. vector coding, when they cannot reach towards a visible target but have to explicitly compute the displacement vector of the hand. Our simulations strongly suggest that our analysis is a reliable tool to detect differences in central visuo-motor processes, unless peripheral noise level exceeds 60% in "Endpoint" and 30% in "Displacement" conditions. "Endpoint" conditions can be used to identify the level of peripheral noise in our data and we estimate it to be between 30% and 40%. Since physical movement characteristics were almost identical in the two experimental tasks, we conclude that our analysis is a valid indicator of how the CNS controls movements in our experiment. Therefore, we conclude that the CNS does not employ a monolithic control system, but that it can change the coordinate system used to

control the limb depending on task demands. Thus, subjects use predominantly endpoint or vector coding, depending in the way visual information relevant for movement production is specified. Based on this finding we suggest that the scientific investigation regarding central visuo-motor processes and visuo-motor transformations should not investigate if the CNS uses endpoint or vector coding to guide the hand, but rather the conditions under which one or the other control strategy is used.

Our traditional analysis of movement endpoints did not reveal any systematic differences between "Endpoint" and "Displacement" conditions, and the distributions were aligned with the direction of movement in all conditions. Yet, our control system analysis reveals a difference in the way movements are controlled in the two tasks. Based on this finding we conclude that shape and orientation of distributions of movement endpoints are not necessarily indicative of the way the CNS plans and controls movements.

We estimate the level of peripheral noise in our data to be between 30% and 40%. Even though our analysis is ambiguous with respect to the exact level of peripheral noise, our findings in combination with other reports in the literature (De Grave et al., 2004; Churchland et al., 2006) nevertheless raise the strong possibility that even in a non-repetitive task the contribution of peripheral noise sources can be substantial. In agreement with Churchland et al. (2006), we therefore suggest that in order to better understand how the CNS transforms visual information into movements, empiric data have to be interpreted in terms of both central and peripheral visuo-motor processes.

In our experiments, we pitched vector coding and endpoint coding models against each other. Our experimental design does not distinguish between head- and eye-centered endpoint coding. Furthermore, we cannot determine the possible involvement of body-centered control mechanisms, because not only the head, but also the body and

shoulder remained stationary throughout the experiment. However, our paradigm can be extended to systematically test the involvement of eye, head and body by introducing systematic shifts of the gaze, head and/or body from trial to trial.

Contribution of perceptual noise to movement variability

One possible factor that we have not yet considered is the potential impact of perceptual noise on observers' movement performance. Suppose, for example that observers' judgments of distances in "Displacement" conditions were less reliable than their judgments of position in "Endpoint" conditions. Other things being equal, we would expect in that case that the perceptual noise would influence the reliability of subjects' hand movements such that variability in "Displacement" conditions would be greater than in "Endpoint" conditions. The results show clearly, however, that there were no significant differences in movement variability between these conditions and average movement endpoints were virtually the same. Thus, it is reasonable to conclude from this finding that the "Displacement" and "Endpoint" conditions had comparable levels of visual perceptual noise.

In addition to visual perceptual noise, distributions of movement endpoints are also affected by perceptual noise that arises for example when head, eye, body and hand position are sensed based on proprioceptive and efferent information. For these noise sources it is also reasonable to assume that they affected "Endpoint" and "Displacement" conditions equally, because there were no differences in movement variability or average movement endpoints between "Endpoint" and "Displacement" conditions.

In conclusion, even though we cannot give exact estimates of the contribution of perceptual and/or peripheral motor noise to movement variability in our experiment, neither of these noise sources is likely to have contributed to the differences in movement coding that were revealed by our control systems analysis.

Relation to previous results

It has been reported previously, that the way visual information is presented, affects errors in movement extent and direction (Messier and Kalaska, 1997). Specifically, errors in movement extent and direction follow the same scaling rule when subjects reach towards a visible target, but they scale independently when subsets have to compute the visual displacement vector. As stated in the introduction, this could be taken as evidence for the use endpoint vs. vector coding in those two conditions. Yet, at the same time, large differences in overall error magnitude in Messier and Kalaska's experiments made a direct comparison between the two conditions difficult because peripheral and perceptual noise represent potential confounds. In the current paper, we used a traditional analysis of movement endpoint distributions to investigate if endpoint distributions differ between the two conditions and we did not find any systematic differences. Thus, we can exclude peripheral and perceptual noise as potential confounds. At the

same time, our control system analysis suggests that subjects use different central visuo-motor processes in the two conditions. Therefore, our data are consistent with the interpretation of Messier and Kalaska's (1997) results given in the introduction.

It has been reported that errors in pointing movements to remembered targets depend on the direction of gaze, suggesting the use of eye centered coordinates to guide the hand towards a remembered location in space. These findings hold for both single hand movements (Henriques et al., 1998) and movement sequences (Sorrento and Henriques, 2008). As mentioned in the introduction, endpoint coding models need to employ visual coordinates that define target location independent from hand position, and eye/head-centered coordinates are typically used. Our finding that subjects use endpoint coding in "Endpoint" conditions is consistent with the finding that gaze shifts induces gaze-dependent pointing errors to remembered targets. At the same time, we predict based on our results that a shift of gaze should not result in gaze-dependent pointing errors to remembered targets, when subjects perform in conditions equivalent to our "Displacement" conditions. The reason for these predictions is that vector coding models need to employ visual coordinates that define the hand displacement vector. Thus, they cannot employ eye-centered coordinates, because the eye-target vector will not match the hand-target vector unless the hand starts at the eye. The effects of gaze shifts on pointing errors to remembered targets in "Displacement" conditions remains to be tested in future experiments.

Sequential hand movements have been used by other researchers in order to investigate how movements are controlled. Two widely cited studies in this context were conducted by Bock and Eckmiller (1986) and Bock and Arnold (1993). In both studies, the authors used a paradigm that required subjects to point open loop to sequences of six to eight targets on each trial. They showed that errors accumulate (Bock and Eckmiller, 1986) and that errors on subsequent movements are correlated (Bock and Arnold, 1993). In an open loop pointing task, errors are expected to correlate, if subjects use vector coding and if subjects do not correct their errors. In contrast, if subjects either correct their errors or use endpoint coding, then the accumulation and correlation of errors should not occur. Van den Dobbelsteen et al. (2001) suggested that the accumulation (and thus correlation) of errors observed by Bock and Arnold (1993) is caused by systematic shifts in hand position that arise when vision of the hand is prevented during sequences of open loop pointing (Wann and Ibrahim, 1992; Brown et al., 2003; Smeets et al., 2006). However, systematic shifts may also arise from error accumulation. Thus, it is difficult to determine if shifts and error accumulation are either cause or effect.

The use of visual feedback in the current experiments should have prevented any systematic shifts in perceived hand position so that errors in successive movements should not have been correlated. In order to test this prediction we applied the regression analysis described by Bock and Arnold (1993, pp 113, 114) to our data in "End-

point" conditions separately for each subject and path. To test if correlations are significantly different from zero, we averaged correlation coefficients separately for errors along and orthogonal to the direction of movement across paths for each subject and applied t-tests (two tailed) to these averages. The analysis reveals that correlations are significantly larger than zero both along the direction of movement ($r=0.3$, $t_{(7)}=5.37$, $P=0.001$) and orthogonal to it ($r=0.18$, $t_{(7)}=5.03$, $P=0.0014$). The correlations we observe are considerably lower than those observed by Bock and Arnold (which are around 0.6), but they differ from zero. The correlation of errors we observe is puzzling and it is not explained by any current model of either endpoint or vector coding for conditions in which subjects receive visual feedback about their current hand position (Feldman, 1966; Polit and Bizzi, 1979; Bizzi et al., 1984; Bock and Eckmiller, 1986; Gordon et al., 1994; Rosenbaum et al., 1995; Rossetti et al., 1995; De Graaf et al., 1996; Desmurget and Prablanc, 1997; Ghez et al., 1997; Vindras and Viviani, 1998; van den Dobbelsteen et al., 2001).

One speculative explanation of the correlations we observe in our subjects' data are that subjects used a hybrid control strategy in "Endpoint" conditions (i.e. 60% endpoint coding, 10% vector coding, 30% peripheral noise), and that the vector component of the movement commands was not completely updated by the visual feedback we provided. Additional research will be required to more clearly resolve this issue.

Visuo-motor processes in 2D vs. 3D

It has been suggested that the CNS may employ different central visuo-motor processes depending on the movement degrees of freedom available (Desmurget et al., 1998). Our analysis in "Endpoint" conditions is similar to one used previously in 3D (van den Dobbelsteen et al., 2001). The analysis used in "Displacement" conditions is a significant extension of that, which is introduced here for the first time. Where comparable, i.e. in "Endpoint" conditions, our results replicate previous findings (van den Dobbelsteen et al., 2001). Since our results obtained in 2D agree well with those obtained in 3D we believe that the CNS uses the same central visuo-motor mechanisms in 2D and 3D. Furthermore, we suggest that differences in the observed distributions of movement endpoints between 3 and 2D are caused by differences in peripheral, rather than central visuo-motor processes. In this context, it remains to be investigated how the results obtained in "Displacement" conditions generalize to 3D.

Changes in peripheral vs. central visuo-motor processes

Is it possible that differences between "Endpoint" and "Displacement" conditions are not caused by differences between central, but by differences in peripheral visuo-motor processes? Physical movement characteristics are the same in the two conditions. Therefore, peripheral noise that arises at the neuro-muscular junction cannot explain performance differences between "Endpoint" and "Dis-

placement" tasks. However, even though peripheral noise itself is the same, it is nevertheless possible that the CNS uses a different control law to deal with the peripheral noise in "Endpoint" and "Displacement" conditions. Thus, even though differences in peripheral noise per se could not explain the results, differences in the control law chosen by the CNS could.

It has been suggested that the CNS is flexible in its choice of laws used to control noise that arises at the neuromuscular junction (Todorov and Jordan, 2002; Todorov, 2004). According to the framework of optimal control (Todorov and Jordan, 2002; Todorov, 2004) an initial planning stage selects higher order goals that are then used to define task relevant errors that determine the choice of error control laws. In our experiment, the task relevant error as instructed to subjects can be considered constant, since in both "Endpoint" and "Displacement" conditions subjects were asked to move their hand as accurately as possible to a location that was located at a certain distance and direction with respect to their current hand position. However, even though the instruction-based task relevant error can be considered constant, it is possible that subjects redefined the task and therefore, that we have different higher order goals in "Endpoint" and "Displacement" conditions. For example, the higher order goal in "Endpoint" conditions could be that the endpoint errors be minimized (i.e. deviations from the trajectory along the way are left uncorrected, as long as they do not increase final position error), whereas the goal in "Displacement" conditions could be that the trajectory be traversed as accurately as possible (i.e. deviations from the trajectory along the way are corrected, even if this leads to an increase in final position error). If we permit a redefinition of higher order goals this way, our results are consistent with the model of optimal control. However, in order to *predict* our results, a model of optimal control would need to incorporate a mechanism that chooses a control law based on the type of visual information that is used to specify the required movement on each trial. It follows that our conclusions about task dependent flexibility remain valid regardless of whether one interprets the results in terms of alternative control laws for peripheral noise or alternative types of movement coding parameters.

REFERENCES

Abrams RA, Meyer DE, Kornblum S (1990) Eye-hand coordination: oculomotor control in rapid aimed limb movements. J Exp Psychol Hum Percept Perform 16:248–267.

Atkeson CG, Hollerbach JM (1985) Kinematic features of unrestrained vertical arm movements. J Neurosci 5:2318–2330.

Bizzi E, Accornero N, Chapple W, Hogan N (1984) Posture control and trajectory formation during arm movement. J Neurosci 4: 2738–2744.

Bock O, Arnold K (1993) Error accumulation and error correction in sequential pointing movements. Exp Brain Res 95:111–117.

Bock O, Eckmiller R (1986) Goal-directed arm movements in absence of visual guidance: evidence for amplitude rather than position control. Exp Brain Res 62:451–458.

Brown LE, Rosenbaum DA, Sainburg LS (2003) Limb position drift: implications for control of posture and movement. J Neurophysiol 90:3105–3118.

Carrozzo M, McIntyre J, Zago M, Lacquaniti F (1999) Viewer-centered and body-centered frames of reference in direct visuomotor transformations. Exp Brain Res 129:201–210.

Churchland MM, Afshar A, Shenoy KV (2006) A central source of movement variability. Neuron 52(6):1085–1096.

De Graaf JB, Denier van der Gon JJ, Sittig AC (1996) Vector coding in slow goal-directed arm movements. Percept Psychophys 58: 587–601.

De Grave DDJ, Brenner E, Smeets JBJ (2004) Illusions as a tool to study the coding of pointing movements. Exp Brain Res 155(1): 56–62.

Desmurget M, Grafton S (2000) Forward Modeling allows feedback control for fast reaching movements. Trends Cogn Sci 4:423–431.

Desmurget M, Prablanc C (1997) Postural control of three dimensional prehension movements. J Neurophysiol 77:452–464.

Desmurget M, Pelisson D, Rossetti Y, Prablanc C (1998) From eye to hand: planning goal-directed movements. Neurosci Biobehav Rev 2:761–788.

Feldman AG (1966) Functional tuning of the nervous system during control of movement or maintenance of a steady posture. III. Mechanographic analysis of the execution by man of the simplest motor tasks. Biophysics 11:766–775.

Fisher NI (1993) Statistical analysis of circular data. New York, NY: Cambridge University Press.

Flanders M, Helms Tillery SI, Soechting JF (1992) Early stages in a sensorimotor transformation. Behav Brain Sci 15:309–362.

Ghez C, Favilla M, Ghilardi MF, Gordon J, Bermejo J, Pullman S (1997) Discrete and continuous planning of hand movements and isometric force trajectories. Exp Brain Res 115:217–233.

Gordon J, Ghilardi MF, Ghez C (1994) Accuracy of planar reaching movements. I. Independence of direction and extent variability. Exp Brain Res 99:97–111.

Hamilton A, Jones KE, Wolpert DM (2004) The scaling of motor noise with muscle strength and motor unit number in humans. Exp Brain Res 157:417–430.

Harris CM, Wolpert DM (1998) Signal-dependent noise determines motor planning. Nature 394:780–784.

Henriques DYP, Klier EM, Lowy D, Crawford JD (1998) Gaze-centered remapping of remembered visual space in an open-loop pointing. J Neurosci 18:1583–1594.

Lacquaniti F, Caminiti R (1998) Visuo-motor transformations for arm reaching. Eur J Neurosci 10:195–203.

McIntyre J, Stratta F, Lacquaniti F (1997) Viewer-centered frame of reference for pointing to memorized targets in three-dimensional space. J Neurophysiol 78:1601–1618.

McIntyre J, Stratta F, Lacquaniti F (1998) Short-term memory for reaching to visual targets: psychophysical evidence for body-centered reference frames. J Neurosci 18:8423–8435.

Messier J, Kalaska JF (1997) Differential effect of task conditions on errors of direction and extent of reaching movements. Exp Brain Res 115:469–478.

Polit A, Bizzi E (1979) Characteristics of motor programs underlying arm movements in monkeys. J Neurophysiol 42:183–194.

Rosenbaum DA, Loukopoulos LD, Meulenbroek RGJ, Vaughan F, Engelbrecht SE (1995) Planning reaches by evaluating stored postures. Psychol Rev 102:28–67.

Rossetti Y, Desmurget M, Prablanc C (1995) Vectorial coding of movement: vision, proprioception or both? J Neurophysiol 74: 457–463.

Simmons G, Demiris Y (2006) Object grasping using the minimum variance model. Biol Cybern 94:393–407.

Smeets JBJ, van den Dobbelsteen JJ, de Grave DDJ, van Beers RJ, Brenner E (2006) Sensory integration does not lead to sensory calibration. Proc Natl Acad Sci U S A 103(49):18781–18786.

Soechting JF, Flanders M (1989A) Sensorimotor representations for pointing to targets in three-dimensional space. J Neurophysiol 62:582–594.

Soechting JF, Flanders M (1989B) Errors in pointing are due to approximations in sensorimotor transformations. J Neurophysiol 62: 595–608.

Soechting JF, Helms Tillery SI, Flanders M (1990) Transformation from head-to shoulder-centred representation of target direction in arm movements. J Cogn Neurosci 2:32–43.

Sorrento GU, Henriques DYP (2008) Reference frame conversions for repeated arm movements. J Neurophysiol 99:2968–2984.

Todorov E, Jordan MI (2002) Optimal feedback control as a theory for motor coordination. Nat Neurosci 5:1226–1235.

Todorov E (2004) Optimality principles in sensorimotor control (review). Nat Neurosci 7(9):907–915.

van Beers RJ, Haggard P, Wolpert DM (2004) The role of execution noise in movement variability. J Neurophysiol 9:1050–1063.

van den Dobbelsteen JJ, Brenner E, Smeets JBJ (2001) Endpoints of arm movements to visual targets. Exp Brain Res 138:279–287.

Vindras P, Viviani P (1998) Frames of reference and control parameters in visuomanual pointing. J Exp Psychol: Hum Percept Perform 24(2):569–591.

Vindras P, Desmurget M, Viviani P (2005) Error parsing in visuomotor pointing reveals independent processing of amplitude and direction. J Neurophysiol 94:1212–1224.

Wann JP, Ibrahim SF (1992) Does limb proprioception drift? Exp Brain Res 91:162–166.

APPENDIX A

Here we explain how we computed displacement errors and how we recombined displacement errors with hand-target vectors from other trials. Displacement errors were computed in terms of amplitude and direction of the observed displacement, d, compared to the hand-target vector, *h-t*, that pointed from the current hand starting position to the target location. Displacement amplitude errors were computed by dividing the observed displacement amplitude by the corresponding hand-target amplitude, i.e. $\varepsilon_A = A_d / A_{h\text{-}t}$. Displacement orientation errors were computed as angular difference in orientation between observed displacement and hand-target vectors, i.e. $\varepsilon_\theta = \theta_d - \theta_{h\text{-}t}$. To recombine displacement errors with hand-target vectors from other trials, amplitude error was multiplied by the amplitude of the new hand-target vector and orientation error was added to the orientation of the new hand-target vector. Coordinates of fictional endpoints are then given by $\cos(\varepsilon_\theta + \theta_{h'\text{-}t})(\varepsilon_A A_{h'\text{-}t}) + x_{h'\text{-}t}$ and $\sin(\varepsilon_\theta + \theta_{h'\text{-}t})(\varepsilon_A A_{h'\text{-}t}) + y_{h'\text{-}t}$, respectively, where $x_{h'\text{-}t}$ and $y_{h'\text{-}t}$ are coordinates of the hand starting position of new hand-target vector. Displacement errors were computed in the same way in "Displacement" conditions. But please note that in "Displacement" conditions, the hand-target vector, *h-t*, was equivalent to the target-to-target vector, *t-t*, or the target displacement vector, respectively, because subjects were instructed to always move over the target displacement from their current position.

APPENDIX B

Here we explain the reason for, and the computation of normalizing observed and fictional displacements before computing their SD_{2D}. If we compute SD_{2D} of displacements that occurred to the same target from various starting points in either "Endpoint" or "Displacement" conditions, the variance of displacements partially depends on variability due to the spatial separation of the different starting points with respect to the target. This in turn is determined by the experimentally designed spatial layout of the target config-

uration. It is easy to see that the more distant the different starting points are to the target and to each other, the larger the spatial variability introduced by experimental layout. If the spatial variability introduced by experimental layout is large compared to the variability introduced by errors in hand movements, the ratio of observed to fictional displacement SD_{2D} will always be close to one, which would bias our analysis towards endpoint coding. The bias is reduced when analyzing single start–endpoint-paths. However, since the variance of starting points for a single path in the "Displacement" condition is always zero, due to the alignment that removes instruction-based errors, we have to invoke multiple starting points to perform our analysis. To overcome the bias in the analysis introduced by variability due to experimental layout, we normalized observed and fictional displacements with respect to their corresponding target-to-target paths before computing their SD_{2D}.

Observed and fictional displacements were normalized by dividing their amplitudes, A_d, by the amplitude of the corresponding target-to-target vector, A_{t-t}, and by computing the angular difference in orientation between the displacement θ_d and the target-to-target vector θ_{t-t}. Normalized displacement coordinates are then given by $\cos(\theta_d - \theta_{t-t})(A_d / A_{t-t})$ and $\sin(\theta_d - \theta_{t-t})(A_d / A_{t-t})$, respectively.

APPENDIX C

Here we describe the implementation of central and peripheral visuo-motor noise models.

Vector coding models assume that the goal state of the hand is determined based on the vector h-t pointing from the hand to the target. Vector h-t has amplitude $A_{h-t}=|h-t|$ and orientation θ_{h-t}. Central error along vector h-t, $\varepsilon_{A.c}$, was modeled as normally distributed with standard deviation $\sigma_{A.c}$ proportional to vector amplitude. Thus, $\sigma_{A.c}=r_{A.c} \times A_{h-t}$ is the length of the major axis of the central error ellipse. Error orthogonal to vector h-t, $\varepsilon_{o.c}$, was modeled as normally distributed with standard deviation $\sigma_{o.c}=\sigma_{A.c}/a_{CentralNoise}$, so that $a_{CentralNoise}$ determines aspect ratio of error ellipses. To retain equal noise magnitude, i.e. ellipse area, for different ellipse aspect ratios, we can multiply each axis of the ellipse by $\sqrt{a_{CentralNoise}}$, such that area is $\pi \times 0.25 \times \sigma^2_{A.c}$. The error ellipse fits into a tangent cone originating at h and with slope of each leg $\pm r_{A.c}\sqrt{a_{CentralNoise}}/2a_{CentralNoise}$. Coordinates of error contaminated goal state, hp, for every trial are given by

$$\begin{bmatrix} \cos(\theta_{h-t}) & -\sin(\theta_{h-t}) \\ \sin(\theta_{h-t}) & \cos(\theta_{h-t}) \end{bmatrix} \begin{bmatrix} \varepsilon_{o.c} \\ \varepsilon_{A.c}+A_{h-t} \end{bmatrix} + \begin{bmatrix} h_x \\ h_y \end{bmatrix}$$

where h_x and h_y are the coordinates of hand starting position h. Assuming zero mean noise, error ellipses are positioned on the (visible or virtual) target t. Ellipse area is determined by $r_{A.c}$ and vector amplitude A_{h-t}, aspect ratio by $a_{CentralNoise}$ and orientation by vector orientation θ_{h-t}. In "Displacement" conditions vector h-t pointing from the hand to the target is the same as the visual displacement vector t-t.

Endpoint coding models assume that the goal state of the hand is determined based on the vector o-t pointing from the subject's cyclopean eye to the target. Vector o-t has amplitude A_{o-t} and orientation θ_{o-t}. We modeled central errors for eye/head coordinates based on the cyclopean eye because the subject's head remained stationary throughout the experiment (we used a chin rest) and because we can assume that subjects shift their gaze to look at the target or target displacement, respectively, on every trial. Thus, the coordinate system is stationary both in eye centered (representation along the line of sight) and head-centered coordinates and the cyclopean eye is a reasonable approximation to both. Central error in eye/head-centered coordinates was modeled in the same fashion as in hand-centered coordinates, with the difference that errors were computed with respect to vector o-t,

instead of vector h-t. Coordinates of error contaminated goal state, hp, for every trial are then given by

$$\begin{bmatrix} \cos(\theta_{o-t}) & -\sin(\theta_{o-t}) \\ \sin(\theta_{o-t}) & \cos(\theta_{o-t}) \end{bmatrix} \begin{bmatrix} \varepsilon_{o.c} \\ \varepsilon_{A.c}+A_{o-t} \end{bmatrix}$$

Assuming zero mean noise, error ellipses are positioned on the (visible or virtual) target t. Ellipse area is determined by $r_{A.c}$ and vector amplitude A_{o-t}, aspect ratio by $a_{CentralNoise}$ and orientation by vector orientation θ_{o-t}. In "Displacement" conditions, target t is obtained by translating the visual displacement vector t-t onto the current hand position. Since visual feedback in "Displacement" conditions was translated with respect to the physical hand position, we assume that this transformation could be achieved based on a proprioceptive estimate of hand position.

Peripheral noise was modeled according to the execution noise characteristics suggested by van Beers et al. (2004). On every trial, the hand moves from its current position h to the desired goal state hp or along vector $h-hp$ with orientation θ_{h-hp} and amplitude $A_{h-hp}=|h-hp|$, respectively. Movement trajectories were observed to be straight in our experiment. Thus, the major axis of the execution error ellipse is expected to be aligned with θ_{h-hp}. Error along the direction of movement, $\varepsilon_{A.p}$, was chosen to be normally distributed with standard deviation $\sigma_{A.p}$ proportional to movement amplitude. Thus, $\sigma_{A.p}=r_{A.p} \times A_{h-hp}$ is the length of the major axis of the error ellipse. Variation of execution noise ellipse aspect ratio with movement direction (van Beers et al., 2004) can be approximated by the function $a_{PeripheralNoise}=0.75(\sin(2\theta_{h-hp})+3)$. This function has maxima of 3 at 45 and 225°, and minima of 1.5 at 135 and 315° and is plotted in Fig. A.

To vary aspect ratio the minor axis of the ellipse was chosen to be $\sigma_{A.p}/a_{PeripheralNoise}$, such that error orthogonal to the direction of movement, $\varepsilon_{o.p}$, was normally distributed with standard deviation $\sigma_{o.p}=\sigma_{A.p}/a_{PeripheralNoise}$. To retain equal noise magnitude, i.e. ellipse area, across changes in movement direction, and thus aspect ratio, we multiply each axis of the ellipse by $\sqrt{a_{PeripheralNoise}}$, such that area is $\pi \times 0.25 \times \sigma^2_{A.p}$. The error ellipse fits into a tangent cone originating at h and with slope of each leg $\pm r_{A.p}\sqrt{a_{PeripheralNoise}}/2a_{PeripheralNoise}$. Thus, the angular spread of execution noise is independent from movement amplitude. Coordinates of execution noise contaminated movement endpoints for every trial are given by
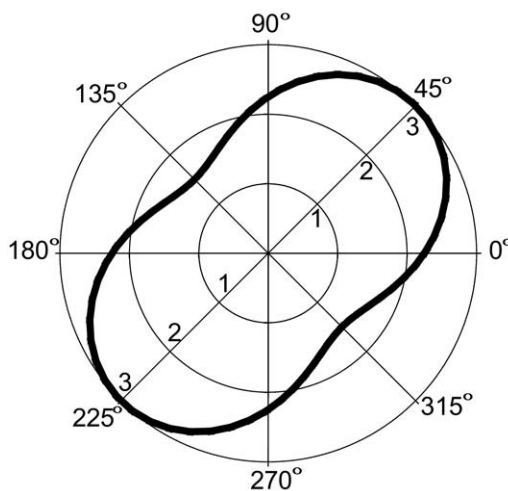

Fig. A. Plot of the function $a_{PeripheralNoise}=0.75(\sin(2\theta_{h-hp})+3)$. This function has maxima of 3 at 45 and 225°, and minima of 1.5 at 135 and 315°. It was used to model movement direction dependent changes in ellipse aspect ratio for execution noise.

$$\begin{bmatrix} \cos(\theta_{h-hp}) & -\sin(\theta_{h-hp}) \\ \sin(\theta_{h-hp}) & \cos(\theta_{h-hp}) \end{bmatrix} \begin{bmatrix} \varepsilon_{o.p} \\ \varepsilon_{A.p} + A_{h-hp} \end{bmatrix} + \begin{bmatrix} h_x \\ h_y \end{bmatrix}$$

where h_x and h_y are the coordinates of hand starting position h. Assuming zero mean noise, error ellipses for execution noise are positioned on planned movement endpoint hp. Ellipse area is determined by $r_{A.p}$ and vector amplitude A_{h-hp}, aspect ratio by $a_{PeripheralNoise}$ and orientation by vector orientation θ_{h-hp}. Note that magnitude and direction of vector h–hp determine execution noise.

Simulation parameters

We simulated central and peripheral noise models at levels from 0% to 100% execution noise, in 10% steps and at overall noise levels of 7.5%, 10% and 15% or base settings of $r_A = 0.075$, 0.1 or 0.15, respectively. In order to keep absolute noise area constant, we scaled $r_{A.c}$ and $r_{A.p}$ accordingly. For example, at total noise level 7.5% ($r_A = 0.075$) and execution noise level 10%, $r_{A.p}$ would be equal to $0.075 \cdot \sqrt{.1}$ and $r_{A.c}$ would be equal to $0.075 \cdot \sqrt{.9}$. Both central noise models were simulated with $a_{CentralNoise}$ set to 2.5, 2, 1.7, 1.3 and 1.

The different geometries of two central noise models, i.e. endpoint and vector coding, result in different absolute noise magnitudes, i.e. ellipse areas, for same values of $r_{A.c}$. For example, subjects' eyes and head are always further away from the stimuli than subjects' hands, such that the amplitude of the eye-target vector generally exceeds the amplitude of the hand-target vector. If we computed errors based on the same noise level $r_{A.c}$ without any additional adjustment, absolute noise magnitude, i.e. ellipse area, would be much larger for endpoint coding, such that peripheral noise would contribute less to endpoint coding than to vector coding models for same values of $r_{A.c}$. Since the two central noise models make different predictions regarding expected error magnitude for different visual targets, it is theoretically unreasonable to equate ellipse areas for individual targets or displacements. Thus, we decided to match average ellipse area between vector and endpoint coding models across all main and filler targets and/or displacements, by introducing a scaling factor for different levels of $r_{A.c}$, for the endpoint coding model.